ASC Report No. 34/2012

Multiscale Modeling in Micromagnetics: Well-Posedness and Numerical Integration

F. Bruckner, M. Feischl, T. Führer, P. Goldenits,
M. Page, D. Praetorius and D. Süss

Institute for Analysis and Scientific Computing
Vienna University of Technology — TU Wien
www.asc.tuwien.ac.at ISBN 978-3-902627-05-6

Most recent ASC Reports

33/2012 *H. Winkler, H. Woracek*
Symmetry in de Branges almost Pontryagin spaces

32/2012 *H. Hofstätter, O. Koch, M. Thalhammer*
Convergence of split-step generalized-Laguerre-Fourier-Hermite methods for Gross-Pitaevskii equations with rotation term

31/2012 *S. Esterhazy and J.M. Melenk*
An analysis of discretizations of the Helmholtz equation in L^2 and in negative norms (extended version)

30/2012 *H. Hofstätter, O. Koch*
An Approximate Eigensolver for Self-Consistent Field Calculations

29/2012 *A. Baranov, H. Woracek*
De Branges' theorem on approximation problems of Bernstein type

28/2012 *B. Schörkhuber, T. Meurer, and A. Jüngel*
Flatness of semilinear parabolic PDEs - A generalized Chauchy-Kowalevski approach

27/2012 *R. Donninger and B. Schörkhuber*
Stable blow up dynamics for energy supercritical wave equations

26/2012 *P. Amodio, C.J. Budd, O. Koch, G. Settanni, E.B. Weinmüller*
Asymptotical Computations for a Model of Flow in Concrete

25/2012 *J.M. Melenk und T. Wurzer*
On the stability of the polynomial L^2-projection on triangles and tetrahedra

24/2012 *P. Amodio, Ch. Budd, O. Koch, G. Settanni, and E.B. Weinmüller*
Numerical Solution of a Second-Order Initial Value Problem Describing Flow in Concrete

Institute for Analysis and Scientific Computing
Vienna University of Technology
Wiedner Hauptstraße 8–10
1040 Wien, Austria

E-Mail: admin@asc.tuwien.ac.at
WWW: http://www.asc.tuwien.ac.at
FAX: +43-1-58801-10196

ISBN 978-3-902627-05-6

ASC
TU WIEN

MULTISCALE MODELING IN MICROMAGNETICS: WELL-POSEDNESS AND NUMERICAL INTEGRATION

F. BRUCKNER, M. FEISCHL, T. FÜHRER, P. GOLDENITS, M. PAGE, D. PRAETORIUS, AND D. SUESS

Abstract. Various applications ranging from spintronic devices, giant magnetoresistance (GMR) sensors, and magnetic storage devices, include magnetic parts on very different length scales. Since the consideration of the Landau-Lifshitz-Gilbert equation (LLG) constrains the maximum element size to the exchange length within the media, it is numerically not attractive to simulate macroscopic parts with this approach. On the other hand, the magnetostatic Maxwell equations do not constrain the element size, but therefore cannot describe the short-range exchange interaction accurately. A combination of both methods allows to describe magnetic domains within the micromagnetic regime by use of LLG and also considers the macroscopic parts by a nonlinear material law using Maxwell's equations. In our work, we prove that under certain assumptions on the nonlinear material law, this multiscale version of LLG admits weak solutions. Our proof is constructive in the sense that we provide a linear-implicit numerical integrator for the multiscale model such that the numerically computable finite element solutions admit weak H^1-convergence —at least for a subsequence— towards a weak solution.

1. Introduction

The understanding of magnetization dynamics, especially on a microscale, is of utter relevance, for example in the development of magnetic sensors, recording heads, and magneto-resistive storage devices. In the literature, a well accepted model for micromagnetic phenomena, is the Landau-Lifshitz-Gilbert equation (LLG), see (13). This nonlinear partial differential equation describes the behaviour of the magnetization of some ferromagnetic body under the influence of a so-called effective field. Existence (and non-uniqueness) of weak solutions of LLG goes back to [3]. As far as numerical simulation is concerned, convergent integrators can be found e.g. in the works [6, 7] or [5], where even coupling to Maxwell's equations is considered. For a complete review, we refer to [9, 13, 20] or the monographs [17, 22] and the references therein. Recently, there has been a major breakthrough in the development of effective and mathematically convergent algorithms for the numerical integration of LLG. In [1], an integrator is proposed which is unconditionally convergent and only needs the solution of one linear system per timestep. The effective field in this work, however, only covers microcrystalline exchange effects and is thus quite restricted. In the subsequent works [2, 14, 15, 16] the analysis for this integrator was widened to cover more general (linear) field contributions while still maintaing unconditional convergence.

In our work, we generalize the integrator from [1] even more and basically allow arbitrary field contributions (Section 3). Under some assumptions on those contributions, namely boundedness and some weak convergence property, cf. (31)–(32), our main theorem still proves unconditional convergence towards some weak solution of LLG (Theorem 7). In particular, our analysis allows to incorporate the approximate solution resp. discretization of effective field contributions like e.g. the strayfield which cannot be computed analytically in practice, but requires certain FEM-BEM coupling methods (Section 4.5). Such additional approximation errors have so far been neglected in the previous works. In particular, we show that the hybrid FEM-BEM approach from [10] for strayfield computations does not affect the unconditional convergence of the proposed integrator (Proposition 17).

From the point of applications, the numerical integration of LLG restricts the maximum element size for the underlying mesh to the (material dependent) exchange length in order to numerically resolve domain wall patterns. Otherwise, the numerical simulation was not able to capture the effects stemming from the exchange term and would lead to qualitatively wrong and even unphysical results. However, due to limited memory, this constraint on the mesh-size practically also imposes a restriction on the actual size of the contemplated ferromagnetic sample. Considering the magnetostatic Maxwell equations combined with a (nonlinear) material law instead, one does not face such a restriction on the mesh-size (and thus on the computational domain). On the one hand, this implies that such a rough model cannot be used to describe short-range interactions like those driving LLG. On the other hand, this gives us the opportunity to cover larger domains and still maintain a managable problem size.

In our work, we show how to combine microscopic and macroscopic domains to end up with an appropriate multiscale problem (Section 2): On the microscopic part, where we aim to simulate the configuration of the magnetization, we solve LLG. The influence of a possible macroscopic part, where the magnetization is not the goal of the computation, is described by means of the magnetostatic Maxwell equations in combination with some (nonlinear) material law. This macroscopic part then gives rise to an additional nonlinear and nonlocal field contribution (Section 4.6) such that unconditional convergence of the numerical integrator or even mere existence of weak solutions in this case is not obvious. For certain practically relevant material laws, we analyze a discretization of the multiscale contribution by means of the Johnson-Nédélec coupling and prove that the proposed numerical integrator still preserves unconditional convergence (Proposition 28).

Outline The remainder of this paper is organized as follows: In Section 2, we give a motivation and the mathematical modeling for our multiscale model. While Section 2.1 focuses on the new contribution to the effective field, Section 2.2 recalls the LLG equation used for the microscopic part. In Section 3, we introduce our numerical integrator in a quite general framework and formulate the main result (Theorem 7) which states unconditional convergence under certain assumptions (31)–(32) on the (discretized) effective field contributions. The remainder of this section is then dedicated to the proof of Theorem 7. In Section 4, we consider different effective field contributions as well as possible discretizations and show that the assumptions of Theorem 7 are satisfied. Our analysis includes general anisotropy densities (Section 4.2) as well as contributions which stem from the solution of operator equations with uniformly monotone operators (Section 4.3). This abstract framework then covers, in particular, the hybrid FEM-BEM discretization from [10] for the strayfield (Section 4.5) as well as the proposed multiscale contribution to the effective field (Section 4.6).

2. Multiscale model

In our model, we consider two separated ferromagnetic bodies Ω_1 and Ω_2 as schematized in Figure 1. Let $\Omega_1, \Omega_2 \subset \mathbb{R}^3$ be bounded Lipschitz domains with Euclidean distance $\mathrm{dist}(\Omega_1, \Omega_2) > 0$ and boundaries $\Gamma_1 = \partial\Omega_1$ resp. $\Gamma_2 = \partial\Omega_2$. On the microscopic part Ω_1, we are interested in the domain configuration and thus solve the Landau-Lifshitz-Gilbert equation (LLG) to obtain the magnetization $\boldsymbol{M}_1 : \Omega_1 \to \mathbb{R}^3$. On Ω_2, we will use the macroscopic Maxwell equations with a (possibly nonlinear) material law instead.

To motivate this setting, we consider a magnetic recording head (see Figures 1 and 2). The microscopic sensor element is based on the giant magnetoresistance (GMR) effect, and it requires the use of LLG in order to describe the short range interactions between the individual layers of the sensor accurately. On the other hand, the smaller these sensor elements, the more important becomes the shielding of the strayfield of neighbouring data bits. In practice, this is achieved by means of some macroscopic softmagnetic shields located directly besides the GMR sensor. Describing these large components by use of LLG would lead to very large problem sizes, because the detailed domain structure within the magnetic shields would be calculated. As proposed in this paper, macroscopic Maxwell equations allow to overcome this limitation and thus provide a profound method to describe the influence of the shields in an averaged sense. While this work focuses on the mathematical model and a possible discretization, we refer to [8] for numerical simulations and the experimental validation of the model proposed.

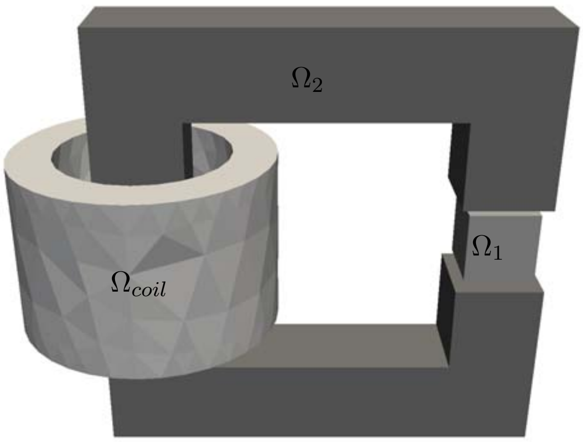

FIGURE 1. Example geometry which demonstrates model separation into LLG region Ω_1 and Maxwell region Ω_2 (and in this case in an electric coil region Ω_{coil}). Here, Ω_1 represents one grain of a recording media and Ω_2 shows a simple model of a recording write head.

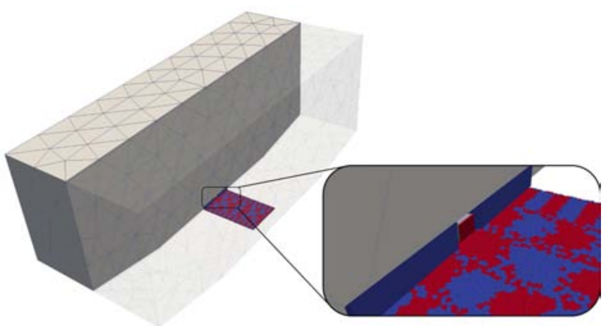

FIGURE 2. The example setup consists of a microscopic GMR sensor element in between two macroscopic shields. Beyond the GMR sensor a magnetic storage media is indicated. The multiscale algorithm is used to calculate the stationary state of the GMR sensor for various applied external fields.

2.1. **Magnetostatic Maxwell equations.** The magnetostatic Maxwell equations read

$$\nabla \times \boldsymbol{H} = \boldsymbol{j} \quad \text{and} \quad \nabla \cdot \boldsymbol{B} = 0 \quad \text{in } \mathbb{R}^3, \tag{1}$$

where $\boldsymbol{H} : \mathbb{R}^3 \to \mathbb{R}^3$ is the magnetic field strength and where the magnetic flux density $\boldsymbol{B} : \mathbb{R}^3 \to \mathbb{R}^3$ is given by

$$\boldsymbol{B} = \mu_0(\boldsymbol{H} + \boldsymbol{M}) \quad \text{in } \mathbb{R}^3 \tag{2}$$

with μ_0 the permeability of vacuum. The current density $\boldsymbol{j}$ is the source of the magnetic field strength $\boldsymbol{H}$. The magnetization field $\boldsymbol{M}$ is non-trivial on the magnetic bodies $\Omega_1 \cup \Omega_2$, but vanishes in $\mathbb{R}^3 \backslash \overline{(\Omega_1 \cup \Omega_2)}$. The total magnetic field is split into

$$\boldsymbol{H} = \boldsymbol{H}_1 + \boldsymbol{H}_2 + \boldsymbol{H}_{\mathrm{app}}, \tag{3}$$

where $\boldsymbol{H}_j : \mathbb{R}^3 \to \mathbb{R}^3$ is the magnetic field induced by the magnetization $\boldsymbol{M}$ on Ω_j and $\boldsymbol{H}_{\mathrm{app}}$ is the field generated by the current density $\boldsymbol{j}$ in $\mathbb{R}^3 \backslash \overline{\Omega_1 \cup \Omega_2}$. This implies

$$\nabla \times \boldsymbol{H}_{\mathrm{app}} = \boldsymbol{j} \quad \text{and therefore} \quad \nabla \times \boldsymbol{H}_j = 0 \quad \text{in } \mathbb{R}^3. \tag{4}$$

In particular, the induced fields are gradient fields $\boldsymbol{H}_j = -\nabla U_j$ with certain scalar potentials $U_j : \mathbb{R}^3 \to \mathbb{R}$. We assume that $\boldsymbol{H}_{\mathrm{app}}$ is induced by currents only, but not by magnetic monopoles. Therefore,

$$\nabla \cdot \boldsymbol{H}_{\mathrm{app}} = 0 \quad \text{in } \mathbb{R}^3. \tag{5}$$

Moreover, the sources of $\boldsymbol{H}_j$ lie inside Ω_j only and hence

$$\nabla \cdot \boldsymbol{H}_j = 0 \quad \text{in } \mathbb{R}^3 \backslash \overline{\Omega}_j. \tag{6}$$

From the magnetic flux $\boldsymbol{B}$, we obtain

$$0 = \nabla \cdot \boldsymbol{B} = \mu_0(\nabla \cdot \boldsymbol{H} + \nabla \cdot \boldsymbol{M}) = \mu_0(\nabla \cdot \boldsymbol{H}_j + \nabla \cdot \boldsymbol{M}) \quad \text{on } \Omega_j. \tag{7}$$

Together with $\boldsymbol{H}_j = -\nabla U_j$ and (6), this reveals

$$\Delta U_j = \nabla \cdot \boldsymbol{M} \quad \text{in } \Omega_j, \tag{8a}$$

$$\Delta U_j = 0 \qquad \text{in } \mathbb{R}^3 \backslash \overline{\Omega}_j. \tag{8b}$$

For the micromagnetic body Ω_1, the respective magnetization $\boldsymbol{M}_1 = \boldsymbol{M}|_{\Omega_1}$ is computed by LLG, see Section 2.2 below. The overall transmission problem (8) is supplemented by boundary conditions as well as a radiation condition and reads

$$\Delta U_1 = \nabla \cdot \boldsymbol{M}_1 \quad \text{in } \Omega_1, \tag{9a}$$

$$\Delta U_1 = 0 \qquad \text{in } \mathbb{R}^3 \backslash \overline{\Omega}_1. \tag{9b}$$

$$U_1^{\mathrm{ext}} - U_1^{\mathrm{int}} = 0 \qquad \text{on } \Gamma_1, \tag{9c}$$

$$\partial_{\boldsymbol{\nu}} U_1^{\mathrm{ext}} - \partial_{\boldsymbol{\nu}} U_1^{\mathrm{int}} = -\boldsymbol{M}_1 \cdot \boldsymbol{\nu} \quad \text{on } \Gamma_1, \tag{9d}$$

$$U_1(x) = \mathcal{O}(1/|x|) \quad \text{as } |x| \to \infty. \tag{9e}$$

Here, the superscripts *int* and *ext* indicate whether the trace is considered from inside Ω_1 (resp. Ω_2 in (12) below) or the exterior domain $\mathbb{R}^3 \backslash \overline{\Omega}_1$ (resp. $\mathbb{R}^3 \backslash \overline{\Omega}_2$ in (12) below). Moreover, $\boldsymbol{\nu}$ denotes the outer unit normal vector on Γ_1 (resp. Γ_2 in (12) below), which points from Ω_1 (resp. Ω_2 in (12) below) to the exterior domain. For the macroscopic body Ω_2, we assume a nonlinear material law

$$\boldsymbol{M} = \chi(|\boldsymbol{H}|)\boldsymbol{H} \quad \text{on } \Omega_2 \tag{10}$$

with a scalar function $\chi : \mathbb{R}_{\geq 0} \to \mathbb{R}$ and $|\cdot|$ the modulus. Some examples for suitable χ are listed below (see Remark 21).

For the computation of the potential U_2, we introduce an auxiliary potential U_{app}. Recall that $\nabla \times \boldsymbol{H}_{\mathrm{app}} = 0$ in Ω_2. If Ω_2 is simply connected, we infer $\boldsymbol{H}_{\mathrm{app}} = -\nabla U_{\mathrm{app}}$ on

Ω_2 with some potential $U_{\text{app}} : \Omega_2 \to \mathbb{R}$. According to (5) and up to an additive constant, U_2 can be obtained as the unique solution of the Neumann problem

$$
\begin{aligned}
\Delta U_{\text{app}} &= 0 && \text{in } \Omega_2, && \text{(11a)}\\
\partial_{\boldsymbol{\nu}} U_{\text{app}}^{\text{int}} &= -\boldsymbol{H}_{\text{app}}^{\text{int}} \cdot \boldsymbol{\nu} && \text{on } \Gamma_2, && \text{(11b)}
\end{aligned}
$$

with $\int_{\Omega_2} U_{\text{app}}\, dx = 0$. The transmission problem for the total potential $U = U_1 + U_2 + U_{\text{app}}$ of the total magnetic field $\boldsymbol{H} = -\nabla U$ in Ω_2 and for the potential U_2 in $\mathbb{R}^3 \backslash \overline{\Omega}_2$, supplemented by a radiation condition, reads

$$
\begin{aligned}
\nabla \cdot \Big((1 + \chi(|\nabla U|)) \nabla U \Big) &= 0 && \text{on } \Omega_2, && \text{(12a)}\\
\Delta U_2 &= 0 && \text{on } \mathbb{R}^3 \backslash \overline{\Omega}_2, && \text{(12b)}\\
U_2^{\text{ext}} - U^{\text{int}} &= -U_1^{\text{int}} - U_{\text{app}}^{\text{int}} && \text{on } \Gamma_2, && \text{(12c)}\\
\partial_{\boldsymbol{\nu}} U_2^{\text{ext}} - (1 + \chi(|\nabla U^{\text{int}}|)) \partial_{\boldsymbol{\nu}} U^{\text{int}} &= (\boldsymbol{H}_1^{\text{ext}} + \boldsymbol{H}_{\text{app}}^{\text{ext}}) \cdot \boldsymbol{\nu} && \text{on } \Gamma_2, && \text{(12d)}\\
U_2(x) &= \mathcal{O}(1/|x|) && \text{as } |x| \to \infty, && \text{(12e)}
\end{aligned}
$$

where (12a) follows from (1)–(6) and (10). The boundary conditions of (12) are derived from (1), which leads to $(\boldsymbol{H}^{\text{ext}} - \boldsymbol{H}^{\text{int}}) \cdot \boldsymbol{\nu} = 0$ on Γ_2, and the continuity of U_2 on Γ_2. Details on computation of the above quantities are postponed to section 4.

Remark 1. *In case of a linear material law $\chi(|\boldsymbol{H}|) = \chi \in \mathbb{R}_{>0}$ in* (10)*, the transmission problem* (12) *simplifies to $(1+\chi)\Delta U_2 = 0$ in Ω_2, $U_2^{\text{ext}} - U_2^{\text{int}} = 0$ on Γ_2, and $\partial_{\boldsymbol{\nu}} U_2^{\text{ext}} - (1+\chi)\partial_{\boldsymbol{\nu}} U_2^{\text{int}} = (\boldsymbol{H}_1^{\text{ext}} + \boldsymbol{H}_{\text{app}}^{\text{ext}}) \cdot \boldsymbol{\nu}$ on Γ_2 in* (12a), (12c)*, and* (12d)*, respectively. In particular, the Neumann problem* (11) *does not have to be solved. Moreover, we do not have to assume that Ω_2 is simply connected.*

2.2. **Landau-Lifshitz-Gilbert equation.** Let $\alpha \geq 0$ denote a dimensionless empiric damping parameter, called Gilbert damping constant, and let the magnetization of the ferromagnetic body Ω_1 be characterized by the vector valued function

$$
\boldsymbol{M}_1 : (0, t_{\text{end}}) \times \Omega_1 \to \Big\{ \boldsymbol{x} \in \mathbb{R}^3 \, : \, |\boldsymbol{x}| = M_s \Big\},
$$

in ampere per meters $[A/m]$ where the constant $M_s > 0$ in $[A/m]$ refers to the saturation magnetization. Then, the Landau-Lifshitz-Gilbert equation reads

$$
\frac{\partial \boldsymbol{M}_1}{\partial t} = -\frac{\gamma_0}{1+\alpha^2} \boldsymbol{M}_1 \times \boldsymbol{H}_{\text{eff}} - \frac{\alpha \gamma_0}{(1+\alpha^2) M_s} \boldsymbol{M}_1 \times (\boldsymbol{M}_1 \times \boldsymbol{H}_{\text{eff}}), \tag{13a}
$$

supplemented by according initial and boundary conditions

$$
\begin{aligned}
\boldsymbol{M}_1(0) &= \boldsymbol{M}^0 && \text{in } \Omega_1, && \text{(13b)}\\
\partial_{\boldsymbol{\nu}} \boldsymbol{M}_1 &= 0 && \text{on } (0, t_{\text{end}}) \times \partial\Omega_1. && \text{(13c)}
\end{aligned}
$$

Here, $\gamma_0 = 2,210173 \cdot 10^5$ in $[m/As]$ denotes the gyromagnetic ratio and $\boldsymbol{M}^0 : \Omega_1 \to \mathbb{R}^3$ with $|\boldsymbol{M}^0| = M_s$ in Ω_1 is a given initial magnetization. The effective field $\boldsymbol{H}_{\text{eff}}$ in $[A/m]$ depends on $\boldsymbol{M}_1$ and the magnetic field strength $\boldsymbol{H}$, and is given as the negative variation of the Gibbs free energy

$$
\boldsymbol{H}_{\text{eff}} = -\frac{\delta E(\boldsymbol{M}_1)}{\delta \boldsymbol{M}_1}. \tag{14}
$$

In this work, the bulk energy $E(\cdot)$ consists of exchange energy, anisotropy energy as well as magnetostatic energy

$$
E(\boldsymbol{M}_1) = \frac{A}{M_s^2} \int_{\Omega_1} |\nabla \boldsymbol{M}_1|^2 + K \int_{\Omega_1} \phi(\boldsymbol{M}_1/M_s)\, dx - \mu_0 \int_{\Omega_1} \boldsymbol{H} \cdot \boldsymbol{M}_1 \, dx, \tag{15}
$$

The exchange constant $A > 0$ in $[J/m]$ and anisotropy constant $K > 0$ in $[J/m^3]$ depend on the ferromagnetic material. Moreover, ϕ refers to the crystalline anisotropy density and $\mu_0 = 4\pi \cdot 10^{-7}[Tm/A]$ denotes the permeability of vacuum. The effective field is thus given by

$$\boldsymbol{H}_{\text{eff}} = \frac{2A}{\mu_0 M_s^2} \Delta \boldsymbol{M}_1 - \frac{K}{\mu_0 M_s^2} D\phi(\boldsymbol{M}_1) + \boldsymbol{H} \quad \text{in } [A/m]. \tag{16}$$

Note that the microscopic LLG equation and the macroscopic Maxwell equations are coupled through the magnetic field strength $\boldsymbol{H}$ and hence through the effective field $\boldsymbol{H}_{\text{eff}}$. Altogether, we will thus solve the multiscale problem by solving LLG on Ω_1 and incorporating the effects of Ω_2 via this coupling.

3. General LLG equation

In this section, we consider the non-dimensional form of LLG with a quite general effective field $\boldsymbol{h}_{\text{eff}}$ which covers the multiscale problem from the previous section. We recall some equivalent formulations of LLG and then state our notion of a weak solution, which has been introduced by Alouges & Soyeur, see [3], for the small-particle limit $\boldsymbol{h}_{\text{eff}} = \Delta \boldsymbol{m}$ and which is now extended to the present situation. We then formulate a linear-implicit time integrator in the spirit of [1, 2, 14, 15, 16].

3.1. **Nondimensional form of LLG.** We set $\boldsymbol{m} := \boldsymbol{M}_1/M_s$, $\boldsymbol{m}^0 := \boldsymbol{M}^0/M_s$, $\boldsymbol{h}_{\text{eff}} := \boldsymbol{H}_{\text{eff}}/M_s$ and perform the substitution $\tau = \gamma_0 M_s t$ with τ being the so-called reduced time. With $\Omega_\tau = [0, \tau_{\text{end}}] \times \Omega_1$ the space-time cylinder and $\boldsymbol{m} : \Omega_\tau \to \mathbb{S} := \left\{x \in \mathbb{R}^3 \,:\, |x| = 1\right\}$ the (sought) magnetization, the nondimensional form of LLG reads

$$\partial_\tau \boldsymbol{m} = -\frac{1}{1+\alpha^2} \boldsymbol{m} \times \boldsymbol{h}_{\text{eff}} - \frac{\alpha}{1+\alpha^2} \boldsymbol{m} \times (\boldsymbol{m} \times \boldsymbol{h}_{\text{eff}}) \tag{17a}$$

supplemented by initial and boundary conditions

$$\boldsymbol{m}(0) = \boldsymbol{m}^0 \quad \text{in } \Omega_1, \tag{17b}$$

$$\partial_{\boldsymbol{\nu}} \boldsymbol{m} = 0 \qquad \text{in } (0,\tau) \times \partial\Omega_1. \tag{17c}$$

The effective field reads

$$\boldsymbol{h}_{\text{eff}} = \frac{2A}{\mu_0 M_s^2} \Delta \boldsymbol{m} - \frac{K}{\mu_0 M_s^2} D\phi(\boldsymbol{m}) + \boldsymbol{f} - \nabla u_1 - \nabla u_2,$$

where u_1 is obtained from (9) with $\boldsymbol{M}_1$ being replaced by $\boldsymbol{m}$ and where u_2 is obtained from (12) with e.g. $\boldsymbol{H}_{\text{app}}$ replaced by $\boldsymbol{f}$, $\boldsymbol{H}_1$ replaced by $-\nabla u_1$ etc. For the nonlinearity χ, we introduce some $\widetilde{\chi}$ in the nondimensional formulation. Details are elaborated in Section 4.6. We stress that the intrinsic unit of this formulation is $[m]$ for the spatial domain $\Omega_1 \subset \mathbb{R}^3$. Moreover, $1/(\gamma_0 M_s)$ corresponds to 1 second.

Remark 2. *Note that* (17a) *implies* $0 = \boldsymbol{m} \cdot \partial_\tau \boldsymbol{m} = \partial_\tau |\boldsymbol{m}|^2/2$, *i.e. the time derivative* $\partial_\tau \boldsymbol{m}$ *belongs to the tangent space of* $\boldsymbol{m}$ *and the modulus constraint* $|\boldsymbol{m}| = 1$ *a.e. in* Ω_τ *also follows from the PDE formulation.*

3.2. **Notation and function spaces involved.** In this brief section, we want to collect necessary notation as well as the relevant spaces that will be used in the remainder of the manuscript. By L^2, we denote the usual Lebesgue space of square integrable functions and by H^1 the Sobolev space of functions in L^2 that additionally admit a weak derivative in

L^2. For vector fields and corresponding spaces, we use bold symbols, e.g. for $\boldsymbol{f} : \Omega_1 \to \mathbb{R}^3$, we write

$$\|\boldsymbol{f}\|^2_{\boldsymbol{L}^2(\Omega_1)} = \sum_{i=1}^{3} \|f_i\|^2_{L^2(\Omega_1)}.$$

For the space-time cylinder Ω_τ, we consider the spaces $L^2(\boldsymbol{L}^2) := L^2\Big([0,\tau_{\mathrm{end}}], \boldsymbol{L}^2(\Omega_1)\Big) = \boldsymbol{L}^2(\Omega_\tau)$, $L^2(\boldsymbol{H}^1) := L^2\Big([0,\tau_{\mathrm{end}}], \boldsymbol{H}^1(\Omega_1)\Big)$, and $\boldsymbol{H}^1(\Omega_\tau)$ which are associated with the norms

$$\begin{aligned}
\|\boldsymbol{f}\|^2_{L^2(\boldsymbol{L}^2)} &:= \|\boldsymbol{f}\|^2_{\boldsymbol{L}^2(\Omega_\tau)} = \int_0^{\tau_{\mathrm{end}}} \|\boldsymbol{f}(t)\|^2_{\boldsymbol{L}^2(\Omega_1)}\, dt,\\
\|\boldsymbol{f}\|^2_{L^2(\boldsymbol{H}^1)} &:= \|\boldsymbol{f}\|^2_{L^2([0,\tau_{\mathrm{end}}],\boldsymbol{H}^1(\Omega_1))} = \int_0^{\tau_{\mathrm{end}}} \|\boldsymbol{f}(t)\|^2_{\boldsymbol{L}^2(\Omega_1)} + \|\nabla \boldsymbol{f}(t)\|^2_{\boldsymbol{L}^2(\Omega_1)}\, dt,\\
\|\boldsymbol{f}\|^2_{\boldsymbol{H}^1(\Omega_\tau)} &= \int_0^{\tau_{\mathrm{end}}} \|\boldsymbol{f}(t)\|^2_{\boldsymbol{L}^2(\Omega_1)} + \|\nabla \boldsymbol{f}(t)\|^2_{\boldsymbol{L}^2(\Omega_1)} + \|\partial_t \boldsymbol{f}(t)\|^2_{\boldsymbol{L}^2(\Omega_1)}\, dt,
\end{aligned}$$

respectively. Finally, we denote by $(\cdot,\cdot)$ the scalar product in $\boldsymbol{L}^2(\Omega_\tau)$ and by $\langle\cdot,\cdot\rangle$ the scalar product in $\boldsymbol{L}^2(\Omega_1)$, respectively. The Euclidean scalar product of vectors $\boldsymbol{x}, \boldsymbol{y} \in \mathbb{R}^3$ is denoted by $\boldsymbol{x}\cdot\boldsymbol{y}$.

3.3. **Equivalent formulations of LLG and weak solution to general LLG.** The dimensionless formulation of LLG that is usually referred to, has already been stated in (17). Supplemented by the same initial and boundary conditions (17b)–(17c), the equation can also equivalently be stated by

$$\alpha \boldsymbol{m}_t + \boldsymbol{m}\times\boldsymbol{m}_t = \boldsymbol{h}_{\mathrm{eff}}(\boldsymbol{m}) - \Big(\boldsymbol{m}\cdot\boldsymbol{h}_{\mathrm{eff}}(\boldsymbol{m})\Big)\boldsymbol{m} \tag{18}$$

and

$$\boldsymbol{m}_t - \alpha\boldsymbol{m}\times\boldsymbol{m}_t = \boldsymbol{h}_{\mathrm{eff}}(\boldsymbol{m})\times\boldsymbol{m}. \tag{19}$$

In this work, (18) is exploited for the construction of our numerical scheme. For the notion of a weak solution, we use the so-called Gilbert formulation (19). A rigorous proof for the equivalence of the above equations can be found e.g. in [14, Section 1.2].

As far as numerical analysis is concerned, our integrator is an extension of that of Alouges, cf. [1], for the small-particle limit with exchange energy only, to the case under consideration. Independently, the preceding works [2, 14] generalized the approach of [1] to an effective field, which consists of exchange energy, strayfield energy, uniaxial anisotropy, and exterior energy, where only the first term is dealt with implicitly, whereas the remaining lower-order terms are treated explicitly. In this work, we extend this approach to certain nonlinear contributions of the effective field. For this purpose, we introduce a general energy contribution $\boldsymbol{\pi}(\cdot,\cdot)$ that depends on the magnetization $\boldsymbol{m}$ and may depend on an additional given quantity $\zeta \in L^2(Y) = L^2([0,\tau_{\mathrm{end}}], Y)$ for some Banach space Y. For the multiscale model from the introduction, ζ will simply be the applied external field $\boldsymbol{f}$, whereas for the strayfield and anisotropy contribution, ζ will vanish. The forthcoming analysis, however, even allows more general ζ. We now write $\boldsymbol{h}_{\mathrm{eff}}$ in the form

$$\boldsymbol{h}_{\mathrm{eff}} = C_{\mathrm{exch}}\Delta\boldsymbol{m} - \boldsymbol{\pi}(\boldsymbol{m},\zeta) + \boldsymbol{f}, \tag{20a}$$

where the exchange contribution and the exterior field $\boldsymbol{f}$ are explicitly given, while strayfield contribution, material anisotropy, and the induced field from the macroscopic part are concluded in the operator $\boldsymbol{\pi}(\cdot,\cdot)$. Our analysis thus particularly includes the case

$$\boldsymbol{\pi}\Big(\boldsymbol{m}(t),\zeta(t)\Big) := \nabla u_1 + C_{\mathrm{ani}}\, D\phi\Big(\boldsymbol{m}(t)\Big) + \nabla u_2, \tag{20b}$$

but also holds true for general contributions $\boldsymbol{\pi}$, which only act on the spatial variable, as long as they fulfill certain properties, i.e. (31)–(32) below. In (20a)–(20b), the constants are given by

$$C_{\text{exch}} := \frac{2A}{\mu_0 M_s^2} \quad \text{resp.} \quad C_{\text{ani}} := \frac{K}{\mu_0 M_s^2}. \tag{20c}$$

With this notation, our notion of a weak solution reads as follows:

Definition 3. *A function $\boldsymbol{m}$ is called a* weak solution *to LLG in Ω_τ, if*

(i) *$\boldsymbol{m} \in \boldsymbol{H}^1(\Omega_\tau)$ with $|\boldsymbol{m}| = 1$ a.e. in Ω_τ and $\boldsymbol{m}(0) = \boldsymbol{m}^0$ in the sense of traces;*

(ii) *For all $\boldsymbol{\phi} \in C^\infty(\Omega_\tau)$, we have*

$$\begin{aligned}\int_{\Omega_\tau} \boldsymbol{m}_t \cdot \boldsymbol{\phi} - \alpha \int_{\Omega_\tau} (\boldsymbol{m} \times \boldsymbol{m}_t) \cdot \boldsymbol{\phi} &= \\ - C_{\text{exch}} \int_{\Omega_\tau} (\nabla \boldsymbol{m} \times \boldsymbol{m}) \cdot \nabla \boldsymbol{\phi} &- \int_{\Omega_\tau} \Big(\boldsymbol{\pi}(\boldsymbol{m}, \zeta) \times \boldsymbol{m}\Big) \cdot \boldsymbol{\phi} + \int_{\Omega_\tau} (\boldsymbol{f} \times \boldsymbol{m}) \cdot \boldsymbol{\phi}\end{aligned} \tag{21}$$

(iii) *for almost all $t \in (0, \tau)$, we have*

$$\|\nabla \boldsymbol{m}(t)\|^2_{L^2(\Omega_1)} + \|\boldsymbol{m}_\tau\|^2_{L^2(\Omega_t)} \le C, \tag{22}$$

for some constant $C > 0$ which depends only on $\boldsymbol{m}^0$ and $\boldsymbol{f}$.

The existence (and non-uniqueness) of weak solutions has first been shown in [3] for the small particle limit, where $\boldsymbol{\pi}(\cdot,\cdot)$ and $\boldsymbol{f}$ are omitted. We stress, however, that our convergence proof is constructive in the sense that the analysis does not only show convergence towards, but also existence of weak solutions without any assumptions on the smoothness of the quantities involved.

Remark 4. *Under certain assumptions on $\boldsymbol{\pi}(\cdot,\cdot)$ and its upcoming discretization $\boldsymbol{\pi}_h(\cdot,\cdot)$, the energy estimate* (22) *can be improved. We refer to Lemma 29 in the appendix.*

3.4. **Linear-implicit integrator.** We discretize the magnetization $\boldsymbol{m}$ and its time derivative $\boldsymbol{v} = \boldsymbol{m}_\tau$ in space by lowest-order Courant finite elements

$$\boldsymbol{\mathcal{V}}_h := \mathcal{S}^1(\mathcal{T}_h^{\Omega_1})^3 = \Big\{\boldsymbol{n}_h : \overline{\Omega}_1 \to \mathbb{R}^3 \text{ continuous } : \boldsymbol{n}_h|_T \text{ affine for all } T \in \mathcal{T}_h^{\Omega_1}\Big\}, \tag{23}$$

where $\mathcal{T}_h^{\Omega_1}$ is a conforming triangulation of Ω_1 into compact and non-degenerate tetrahedra $T \in \mathcal{T}_h^{\Omega_1}$ with spatial mesh-size h . Let $\mathcal{N}_h$ denote the set of nodes of $\mathcal{T}_h^{\Omega_1}$. For fixed time τ_j, the discrete magnetization is sought in the convex set

$$\boldsymbol{m}(\tau_j) \approx \boldsymbol{m}_h^j \in \boldsymbol{\mathcal{M}}_h := \Big\{\boldsymbol{n}_h \in \boldsymbol{\mathcal{V}}_h \,:\, |\boldsymbol{n}_h(z)| = 1 \text{ for all nodes } z \in \mathcal{N}_h\Big\}, \tag{24}$$

whereas the discrete time derivative is sought in the discrete tangent space

$$\boldsymbol{v}(\tau_j) \approx \boldsymbol{v}_h^j \in \boldsymbol{\mathcal{K}}_{\boldsymbol{m}_h^j} := \Big\{\boldsymbol{n}_h \in \boldsymbol{\mathcal{V}}_h \,:\, \boldsymbol{n}_h(z) \cdot \boldsymbol{m}_h^j(z) = 0 \text{ for all nodes } z \in \mathcal{N}_h\Big\}. \tag{25}$$

For time discretization, we impose a uniform partition $\mathcal{I}_k$ with $0 = \tau_0 < \tau_1 < \ldots < \tau_N = \tau_{\text{end}}$ of the time interval $[0, \tau_{\text{end}}]$. The time step is denoted by $k = k_j := \tau_{j+1} - \tau_j$ for $j = 0, \ldots, N-1$, i.e. $\tau_j = jk$.

We assume that $\boldsymbol{\pi}$ is a spatial operator which maps the magnetization $\boldsymbol{m}(\tau) \in \boldsymbol{L}^2(\Omega_1)$ and $\zeta(\tau) \in Y$ at given time t to some field $\Big(\boldsymbol{\pi}(\boldsymbol{m}, \zeta)\Big)(\tau) = \boldsymbol{\pi}\Big(\boldsymbol{m}(\tau), \zeta(\tau)\Big) \in \boldsymbol{L}^2(\Omega_1)$. For given $h > 0$, let $\boldsymbol{\pi}_h$ be a numerical realization which maps $\boldsymbol{m}(\tau_j) \approx \boldsymbol{m}_h^j \in \boldsymbol{\mathcal{M}}_h$ and $\zeta(\tau_j) \approx \zeta_h^j$ to some $\boldsymbol{\pi}_h(\boldsymbol{m}_h^j, \zeta_h^j) \in \boldsymbol{L}^2(\Omega_1)$. Finally, let $\boldsymbol{f}_h^j$ be an approximation of $\boldsymbol{f}(\tau_j)$ specified below. Then, our numerical time integrator reads as follows:

Algorithm 5. INPUT*: Initial approximation $\boldsymbol{m}_h^0 \in \boldsymbol{\mathcal{M}}_h$ and Gilbert damping parameter $\alpha > 0$, parameter $\theta \in [0,1]$. Then, for $i = 0, 1, 2, \dots, N-1$ do:*

(i) *Compute $\boldsymbol{v}_h^i \in \boldsymbol{\mathcal{K}}_{\boldsymbol{m}_h^i}$ such that for all $\boldsymbol{\psi}_h \in \boldsymbol{\mathcal{K}}_{\boldsymbol{m}_h^i}$ holds*

$$\begin{aligned}\alpha \int_{\Omega_1} \boldsymbol{v}_h^i \cdot \boldsymbol{\psi}_h + C_{\text{exch}}\, k\theta \int_{\Omega_1} \nabla \boldsymbol{v}_h^i \cdot \nabla \boldsymbol{\psi}_h + \int_{\Omega_1} (\boldsymbol{m}_h^i \times \boldsymbol{v}_h^i) \cdot \boldsymbol{\psi}_h \\ = -C_{\text{exch}} \int_{\Omega_1} \nabla \boldsymbol{m}_h^i \cdot \nabla \boldsymbol{\psi}_h - \int_{\Omega_1} \boldsymbol{\pi}_h(\boldsymbol{m}_h^i, \zeta_h^i) \cdot \boldsymbol{\psi}_h + \int_{\Omega_1} \boldsymbol{f}_h^i \cdot \boldsymbol{\psi}_h.\end{aligned} \tag{26}$$

(ii) *Define $\boldsymbol{m}_h^{i+1} \in \boldsymbol{\mathcal{M}}_h$ by $\boldsymbol{m}_h^{i+1}(z) = \dfrac{\boldsymbol{m}_h^i(z) + k\boldsymbol{v}_h^i(z)}{|\boldsymbol{m}_h^i(z) + k\boldsymbol{v}_h^i(z)|}$ for all nodes $z \in \mathcal{N}_h$.*

OUTPUT: *Discrete time derivatives $\boldsymbol{v}_h^i$ and magnetizations $\boldsymbol{m}_h^{i+1}$, for $i \geq 0$.*

Lemma 6. *Algorithm 5 is well-defined, and the definitions*

$$\boldsymbol{m}_{hk}(\tau, x) := \frac{\tau - ik}{k} \boldsymbol{m}_h^{i+1}(x) + \frac{(i+1)k - \tau}{k} \boldsymbol{m}_h^i(x) \tag{27}$$

$$\boldsymbol{m}_{hk}^-(\tau, x) := \boldsymbol{m}_h^i(x), \quad \boldsymbol{m}_{hk}^+(\tau, x) := \boldsymbol{m}_h^{i+1}(x), \tag{28}$$

for $x \in \Omega_1$ and $\tau_i \leq \tau < \tau_{i+1}$ provide discrete magnetizations $\boldsymbol{m}_{hk} \in \mathcal{S}^1(\mathcal{I}_k; \boldsymbol{\mathcal{V}}_h) \subset \boldsymbol{H}^1(\Omega_\tau)$ and $\boldsymbol{m}_{hk}^\pm \in \mathcal{P}^0(\mathcal{I}_k; \boldsymbol{\mathcal{V}}_h) \subset L^2(\boldsymbol{H}^1)$ with $\|\boldsymbol{m}_{hk}\|_{\boldsymbol{L}^\infty(\Omega_\tau)} = \|\boldsymbol{m}_{hk}^\pm\|_{\boldsymbol{L}^\infty(\Omega_\tau)} = 1$, which are continuous and piecewise affine in time (denoted by $\mathcal{S}^1$) resp. piecewise constant in time (denoted by $\mathcal{P}^0$).

Proof. Problem (26) can be rewritten as: *Find $\boldsymbol{v}_h^i \in \boldsymbol{\mathcal{K}}_{\boldsymbol{m}_h^i}$, such that*

$$a(\boldsymbol{v}_h^i, \boldsymbol{\psi}_h) + b^i(\boldsymbol{v}_h^i, \boldsymbol{\psi}_h) = L^i(\boldsymbol{\psi}_h),$$

with

$$\begin{aligned} a(\boldsymbol{\phi}_h, \boldsymbol{\psi}_h) &= \alpha \int_{\Omega_1} \boldsymbol{\phi}_h \cdot \boldsymbol{\psi}_h + C_{\text{exch}} \theta k \int_{\Omega_1} \nabla \boldsymbol{\phi}_h \cdot \nabla \boldsymbol{\psi}_h \\ b^i(\boldsymbol{\phi}_h, \boldsymbol{\psi}_h) &= \int_{\Omega_1} (\boldsymbol{m}_h^i \times \boldsymbol{\phi}_h) \cdot \boldsymbol{\psi}_h \\ L^i(\boldsymbol{\psi}_h) &= -C_{\text{exch}} \int_{\Omega_1} \nabla \boldsymbol{m}_h^i \cdot \nabla \boldsymbol{\psi}_h - \int_{\Omega_1} \boldsymbol{\pi}_h(\boldsymbol{m}_h^i, \zeta_h^i) \cdot \boldsymbol{\psi}_h + \int_{\Omega_1} \boldsymbol{f}_h^i \cdot \boldsymbol{\psi}_h. \end{aligned}$$

For fixed $k > 0, \alpha > 0$, and $\theta > 0$, the bilinear form $a(\cdot,\cdot)$ is equivalent to the $\boldsymbol{H}^1$-scalar product. Moreover, the bilinear form $b(\cdot,\cdot)$ is skew symmetric and hence $b(\boldsymbol{\phi}_h, \boldsymbol{\phi}_h) = 0$. Altogether, $a(\cdot,\cdot) + b(\cdot,\cdot)$ thus is a positive definite bilinear form on the finite dimensional space $\boldsymbol{\mathcal{K}}_{\boldsymbol{m}_h^i}$. Therefore, (26) admits a unique solution $\boldsymbol{v}_h^i \in \boldsymbol{\mathcal{K}}_{\boldsymbol{m}_h^i}$ in each step of the iteration. By definition of the discrete tangent space of $\boldsymbol{m}_h^i$ it holds $|\boldsymbol{m}_h^i + k\boldsymbol{v}_h^i|^2 = 1 + k^2\,|\boldsymbol{v}_h^i|^2 \geq 1$ nodewise. Therefore, the normalization step in the above algorithm is well-defined. By use of barycentric coordinates, an elementary calculation finally proves the pointwise estimates $|\boldsymbol{m}_{hk}(\tau, \boldsymbol{x})|, |\boldsymbol{m}_{hk}^\pm(\tau, \boldsymbol{x})| \leq 1$, see e.g. [1]. □

3.5. **Main theorem.** The following theorem is the main result of this work. It states convergence of the numerical integrator towards a weak solution of the general LLG equation and hence, in particular, mathematical well-posedness of the problem. Afterwards, we will show that the operator $\boldsymbol{\pi}$ and its discretization $\boldsymbol{\pi}_h$ of the multiscale LLG equation satisfy the general assumptions posed. In particular, the concrete problem is thus covered by the general approach.

Theorem 7. ***(a)*** *Let $\theta \in (1/2, 1]$ and suppose that the spatial meshes $\mathcal{T}_h^{\Omega_1}$ are uniformly shape regular and satisfy the angle condition*

$$\int_{\Omega_1} \nabla \eta_i \cdot \nabla \eta_j \leq 0 \quad \text{for all basis functions } \eta_i, \eta_j \in \mathcal{S}^1(\mathcal{T}_h^{\Omega_1}) \text{ with } i \neq j. \tag{29}$$

Define functions $\boldsymbol{f}_{hk}^- \in \mathcal{P}^0\Big(\mathcal{I}_k; \boldsymbol{L}^2(\Omega_1)\Big)$ and $\zeta_{hk}^- \in \mathcal{P}^0(\mathcal{I}_k; Y)$ by $\boldsymbol{f}_{hk}^-(\tau) := \boldsymbol{f}_h^j$, $\zeta_{hk}^-(\tau) := \zeta_h^j$ for $\tau_j \leq \tau < \tau_{j+1}$. We suppose that

$$\boldsymbol{f}_{hk}^- \rightharpoonup \boldsymbol{f} \qquad \text{weakly convergent in } \boldsymbol{L}^2(\Omega_\tau) \tag{30}$$

Moreover, we suppose that the spatial discretization $\boldsymbol{\pi}_h(\cdot,\cdot)$ of $\boldsymbol{\pi}(\cdot,\cdot)$ satisfies

$$\|\boldsymbol{\pi}_h(\boldsymbol{n}, y)\|_{\boldsymbol{L}^2(\Omega_1)} \leq C_1 \tag{31}$$

for all $h, k > 0$ and all $\boldsymbol{n} \in \boldsymbol{L}^2(\Omega_1)$ with $|\boldsymbol{n}| \leq 1$ almost everywhere in Ω_1 and $y \in Y$ with $\|y\|_Y \leq C_2$ for some y-independent constant $C_2 > 0$. Here, $C_1 > 0$ denotes a constant that is independent of $h, k, \boldsymbol{n}$, and y, but may depend on C_2 and Ω_1. We further assume $\|\zeta_h^j\|_Y \leq C_2$ for all $j = 1, \ldots, N$. Under these assumptions, we have strong $\boldsymbol{L}^2(\Omega_\tau)$-subconvergence of $\boldsymbol{m}_{hk}^-$ towards some function $\boldsymbol{m}$.

(b) *In addition to the above, we assume $\boldsymbol{m}_h^0 \rightharpoonup \boldsymbol{m}^0$ weakly in $\boldsymbol{L}^2(\Omega)$ and*

$$\boldsymbol{\pi}_h(\boldsymbol{m}_{hk}^-, \zeta_{hk}^-) \rightharpoonup \boldsymbol{\pi}(\boldsymbol{m}, \zeta) \quad \text{weakly subconvergent in } \boldsymbol{L}^2(\Omega_\tau). \tag{32}$$

Then, the computed FE solutions $\boldsymbol{m}_{hk}$ are weakly subconvergent in $\boldsymbol{H}^1(\Omega_\tau)$ to a weak solution $\boldsymbol{m} \in \boldsymbol{H}^1(\Omega_\tau)$ of general LLG.

Remark 8. (i) *Suppose that the applied exterior field is continuous in time, i.e. $\boldsymbol{f} \in C([0,\tau]; \boldsymbol{L}^2(\Omega_1))$. Let $\boldsymbol{f}_h^j = \boldsymbol{f}(\tau_j)$ denote the evaluation of $\boldsymbol{f}$ at time τ_j. Then, assumption* (30) *is satisfied since $\boldsymbol{f}_{hk}^- \to \boldsymbol{f}$ strongly in $L^\infty(\boldsymbol{L}^2)$.*
(ii) *Suppose that the applied exterior field is continuous in space-time, i.e. $\boldsymbol{f} \in C(\overline{\Omega}_\tau)$. Let $\boldsymbol{f}_h^j$ denote the nodal interpolant of $\boldsymbol{f}(\tau_j) \in C(\overline{\Omega}_1)$ in space. Then, assumption* (30) *is satisfied since $\boldsymbol{f}_{hk}^- \to \boldsymbol{f}$ strongly in $\boldsymbol{L}^\infty(\Omega_\tau)$.*
(iii) *Suppose ζ is continuous in time, i.e. $\zeta \in C([0,\tau], Y)$ and let $\zeta_h^j = \zeta(\tau_j)$ denote the evaluation of ζ at time τ_j. Then, we have $\zeta_{hk}^- \to \zeta$ strongly in $L^\infty(Y)$ and $\|\zeta_h^j\|_Y \leq$* $\sup_{t \in [0,\tau]} \|\zeta(\tau)\|_Y =: \widetilde{C}$.

Remark 9. *The angle condition* (29) *is a technical but crucial ingredient for the convergence analysis. It is automatically fulfilled for tetrahedral meshes with dihedral angles that are smaller than $\pi/2$. If the condition is satisfied by the initial mesh $\mathcal{T}_0$, it can be ensured for the refined meshes as well, provided that, for instance, the mesh refinement strategy from* [28, Section 4.1] *is used.*

In the following, we aim to prove Theorem 7. For sake of readability, the proof is split into three lemmata that roughly cover the following steps:

(i) Boundedness of the discrete quantities and energies.
(ii) Existence of weakly convergent subsequences.
(iii) Identification of the limits with weak solutions of LLG.

Lemma 10. *The discrete quantities $\boldsymbol{m}_h^j$ and $\boldsymbol{v}_h^j$ fulfill the energy estimate*

$$\|\nabla \boldsymbol{m}_h^j\|_{\boldsymbol{L}^2(\Omega_1)}^2 + C_1 k \sum_{i=0}^{j-1} \|\boldsymbol{v}_h^i\|_{\boldsymbol{L}^2(\Omega_1)}^2 + (\theta - 1/2) k^2 \sum_{i=0}^{j-1} \|\nabla \boldsymbol{v}_h^i\|_{\boldsymbol{L}^2(\Omega_1)}^2 \leq \|\nabla \boldsymbol{m}_h^0\|_{\boldsymbol{L}^2(\Omega_1)}^2 + C_2 \tag{33}$$

for some h and k independent constant $C_1, C_2 > 0$ and for any $j = 0, \dots, N$.

Proof. In (26), we use the special test function $\boldsymbol{\psi}_h = \boldsymbol{v}_h^i \in \boldsymbol{\mathcal{K}}_{\boldsymbol{m}_h^i}$ and get

$$\alpha\langle \boldsymbol{v}_h^i, \boldsymbol{v}_h^i\rangle + \underbrace{\Big\langle(\boldsymbol{m}_h^i \times \boldsymbol{v}_h^i), \boldsymbol{v}_h^i)\Big\rangle}_{=0} = -C_{\mathrm{exch}}\Big\langle\nabla(\boldsymbol{m}_h^i + \theta k \boldsymbol{v}_h^i), \nabla \boldsymbol{v}_h^i\Big\rangle + \langle \boldsymbol{f}_h^i, \boldsymbol{v}_h^i\rangle - \Big\langle \boldsymbol{\pi}_h(\boldsymbol{m}_h^i, \zeta_h^i), \boldsymbol{v}_h^i\Big\rangle$$

whence

$$\alpha\|\boldsymbol{v}_h^i\|^2_{\boldsymbol{L}^2(\Omega_1)} + C_{\mathrm{exch}}\theta\, k\|\nabla \boldsymbol{v}_h^i\|^2_{\boldsymbol{L}^2(\Omega_1)} = -C_{\mathrm{exch}}\langle\nabla \boldsymbol{m}_h^i, \nabla \boldsymbol{v}_h^i\rangle + \langle \boldsymbol{f}_h^i, \boldsymbol{v}_h^i\rangle - \Big\langle \boldsymbol{\pi}_h(\boldsymbol{m}_h^i, \zeta_h^i), \boldsymbol{v}_h^i\Big\rangle.$$

Exploiting the angle condition (29), we see that $\|\nabla \boldsymbol{m}_h^{i+1}\|^2_{\boldsymbol{L}^2(\Omega_1)} \le \|\nabla(\boldsymbol{m}_h^i + k\boldsymbol{v}_h^i)\|^2_{\boldsymbol{L}^2(\Omega_1)}$, cf. [1, 2, 14] and thus get

$$\begin{aligned}\frac{1}{2}\|\nabla \boldsymbol{m}_h^{i+1}\|^2_{\boldsymbol{L}^2(\Omega_1)} &\le \frac{1}{2}\|\nabla \boldsymbol{m}_h^i\|^2_{\boldsymbol{L}^2(\Omega_1)} + k\langle\nabla \boldsymbol{m}_h^i, \nabla \boldsymbol{v}_h^i\rangle + \frac{k^2}{2}\|\nabla \boldsymbol{v}_h^i\|^2_{\boldsymbol{L}^2(\Omega_1)}\\ &\le \frac{1}{2}\|\nabla \boldsymbol{m}_h^i\|^2_{\boldsymbol{L}^2(\Omega_1)} - (\theta - 1/2)k^2\|\nabla \boldsymbol{v}_h^i\|^2_{\boldsymbol{L}^2(\Omega_1)} \\ &\quad - \frac{\alpha\, k}{C_{\mathrm{exch}}}\|\boldsymbol{v}_h^i\|^2_{\boldsymbol{L}^2(\Omega_1)} + \frac{k}{C_{\mathrm{exch}}}\langle \boldsymbol{f}_h^i, \boldsymbol{v}_h^i\rangle - \frac{k}{C_{\mathrm{exch}}}\Big\langle \boldsymbol{\pi}_h(\boldsymbol{m}_h^i, \zeta_h^i), \boldsymbol{v}_h^i\Big\rangle.\end{aligned} \tag{34}$$

Next, we sum up over $i = 0, \dots, j-1$ to see

$$\begin{aligned}\frac{1}{2}\|\nabla \boldsymbol{m}_h^j\|^2_{\boldsymbol{L}^2(\Omega_1)} \le \frac{1}{2}\|\nabla \boldsymbol{m}_h^0\|^2_{\boldsymbol{L}^2(\Omega_1)} - (\theta - 1/2)k^2\sum_{i=0}^{j-1}\|\nabla \boldsymbol{v}_h^i\|^2_{\boldsymbol{L}^2(\Omega_1)} - \frac{\alpha k}{C_{\mathrm{exch}}}\sum_{i=0}^{j-1}\|\boldsymbol{v}_h^i\|^2_{\boldsymbol{L}^2(\Omega_1)}\\ + \frac{k}{C_{\mathrm{exch}}}\sum_{i=0}^{j-1}\Big(\langle \boldsymbol{f}_h^i, \boldsymbol{v}_h^i\rangle - \Big\langle \boldsymbol{\pi}_h(\boldsymbol{m}_h^i, \zeta_h^i), \boldsymbol{v}_h^i\Big\rangle\Big).\end{aligned}$$

Using the inequalities of Young and Hölder, this can be further estimated by

$$\begin{aligned}&\frac{1}{2}\|\nabla \boldsymbol{m}_h^j\|^2_{\boldsymbol{L}^2(\Omega_1)} + \frac{k}{C_{\mathrm{exch}}}(\alpha - \varepsilon)\sum_{i=0}^{j-1}\|\boldsymbol{v}_h^i\|^2_{\boldsymbol{L}^2(\Omega_1)}\\ &\quad\le \frac{1}{2}\|\nabla \boldsymbol{m}_h^0\|^2_{\boldsymbol{L}^2(\Omega_1)} - (\theta - 1/2)k^2\sum_{i=0}^{j-1}\|\nabla \boldsymbol{v}_h^i\|^2_{\boldsymbol{L}^2(\Omega_1)}\\ &\qquad + \frac{k}{4C_{\mathrm{exch}}\varepsilon}\sum_{i=0}^{j-1}\Big(\|\boldsymbol{f}_h^i\|^2_{\boldsymbol{L}^2(\Omega_1)} + \|\boldsymbol{\pi}_h(\boldsymbol{m}_h^i, \zeta_h^i)\|^2_{\boldsymbol{L}^2(\Omega_1)}\Big)\\ &\quad\le \frac{1}{2}\|\nabla \boldsymbol{m}_h^0\|^2_{\boldsymbol{L}^2(\Omega_1)} - (\theta - 1/2)k^2\sum_{i=0}^{j-1}\|\nabla \boldsymbol{v}_h^i\|^2_{\boldsymbol{L}^2(\Omega_1)} + C,\end{aligned}$$

for any $\varepsilon > 0$. Here, we have used the boundedness of $\|\boldsymbol{\pi}_h(\boldsymbol{m}_h^i, \zeta_h^i)\|^2_{\boldsymbol{L}^2(\Omega_1)}$, as well as the boundedness of $\|\boldsymbol{f}_{hk}^-\|^2_{\boldsymbol{L}^2(\Omega_1)}$ which holds due to the convergence in (30). Choosing $\varepsilon < \alpha$ concludes the proof. $\square$

Using this energy estimate, we immediately conclude the existence of weakly convergent subsequences. So far, we have only used boundedness of $\boldsymbol{\pi}$ resp. $\boldsymbol{\pi}_h$, i.e. (31). The upcoming statement thus holds independently of (32) and concludes the proof of Theorem 7 (*a*).

Lemma 11. *In addition and analogously to* (27)–(28)*, we define a function $\boldsymbol{v}_{hk}^-$ by*

$$\boldsymbol{v}_{hk}^-(\tau, \boldsymbol{x}) := \boldsymbol{v}_h^j(\boldsymbol{x}) \qquad \text{for } \tau \in [\tau_j, \tau_{j+1}). \tag{35}$$

Then, there exist functions $\boldsymbol{m} \in \boldsymbol{H}^1(\Omega_\tau)$ *and* $\boldsymbol{v} \in \boldsymbol{L}^2(\Omega_\tau)$ *such that*

$$\begin{aligned}
&\boldsymbol{m}_{hk}, \boldsymbol{m}_{hk}^{\pm} \rightharpoonup \boldsymbol{m} \text{ in } \boldsymbol{L}^2(\boldsymbol{H}^1(\Omega_1)), \quad \boldsymbol{m}_{hk} \rightharpoonup \boldsymbol{m} \text{ in } \boldsymbol{H}^1(\Omega_\tau)\\
&\boldsymbol{m}_{hk}, \boldsymbol{m}_{hk}^{\pm} \to \boldsymbol{m} \text{ in } \boldsymbol{L}^2(\Omega_\tau)\\
&\boldsymbol{v}_{hk}^{-} \rightharpoonup \boldsymbol{v} \text{ in } \boldsymbol{L}^2(\Omega_\tau)
\end{aligned} \tag{36}$$

as $(h,k) \to (0,0)$ *independently of each other. Here, the convergence is to be understood for one particular subsequence that is successively constructed.*

Proof. From the boundedness of the discrete quantities, i.e. Lemma 10 for $\theta \in [1/2, 1]$, we immediately get weakly convergent subsequences of all of those sequences. It thus only remains to show, that the limits coincide, i.e.

$$\lim \boldsymbol{m}_{hk}^{+} = \lim \boldsymbol{m}_{hk}^{-} = \lim \boldsymbol{m}_{hk} = \boldsymbol{m} \text{ in } \boldsymbol{L}^2(\Omega_\tau), \boldsymbol{L}^2(\boldsymbol{H}^1),$$

where $\boldsymbol{m} := \lim \boldsymbol{m}_{hk}$ in $\boldsymbol{H}^1(\Omega_\tau)$. By definition, $\boldsymbol{m}_{hk}$ converges to $\boldsymbol{m}$ in $\boldsymbol{L}^2(\Omega_\tau)$ as well as $\boldsymbol{L}^2(\boldsymbol{H}^1)$. Due to the Rellich compactness theorem, the convergence in $\boldsymbol{L}^2(\Omega_\tau)$ is even strong. As for the piecewise constant approximations, we rewrite $\boldsymbol{m}_{hk}$ for $\tau \in [\tau_j, \tau_{j+1})$ as

$$\boldsymbol{m}_{hk} = \boldsymbol{m}_h^j + \frac{\tau - \tau_j}{k}(\boldsymbol{m}_h^{j+1} - \boldsymbol{m}_h^j)$$

to see

$$\begin{aligned}
\|\boldsymbol{m}_{hk} - \boldsymbol{m}_{hk}^{-}\|_{\boldsymbol{L}^2(\Omega_\tau)}^2 &= \sum_{j=0}^{N-1} \int_{\tau_j}^{\tau_{j+1}} \|\boldsymbol{m}_h^j + \frac{\tau - \tau_j}{k}(\boldsymbol{m}_h^{j+1} - \boldsymbol{m}_h^j) - \boldsymbol{m}_h^j\|_{\boldsymbol{L}^2(\Omega_1)}^2\\
&\leq \sum_{j=0}^{N-1} \int_{\tau_j}^{\tau_{j+1}} k^2 \|\frac{\boldsymbol{m}_h^{j+1} - \boldsymbol{m}_h^j}{k}\|_{\boldsymbol{L}^2(\Omega_1)}^2\\
&\lesssim \sum_{j=0}^{N-1} \int_{\tau_j}^{\tau_{j+1}} k^2 \|\boldsymbol{v}_h^j\|_{\boldsymbol{L}^2(\Omega_1)}^2\\
&= k^3 \sum_{j=0}^{N-1} \|\boldsymbol{v}_h^j\|_{\boldsymbol{L}^2(\Omega_1)}^2 \to 0.
\end{aligned}$$

Here, we have used

$$\left| \frac{\boldsymbol{m}_h^{j+1} - \boldsymbol{m}_h^j}{k} \right| \leq |\boldsymbol{v}_h^j|$$

which follows from geometric considerations, see [1, 2], and [14]. Analogously, we get

$$\begin{aligned}
\|\boldsymbol{m}_{hk} - \boldsymbol{m}_{hk}^{+}\|_{\boldsymbol{L}^2(\Omega_\tau)}^2 &= \sum_{j=0}^{N-1} \int_{\tau_j}^{\tau_{j+1}} \|\boldsymbol{m}_h^j + \frac{\tau - \tau_j}{k}(\boldsymbol{m}_h^{j+1} - \boldsymbol{m}_h^j) - \boldsymbol{m}_h^{j+1}\|_{\boldsymbol{L}^2(\Omega_1)}^2\\
&\leq \sum_{j=0}^{N-1} \int_{\tau_j}^{\tau_{j+1}} 4k^2 \|\frac{\boldsymbol{m}_h^{j+1} - \boldsymbol{m}_h^j}{k}\|_{\boldsymbol{L}^2(\Omega_1)}^2\\
&\lesssim k^3 \sum_{j=0}^{N-1} \|\boldsymbol{v}_h^j\|_{\boldsymbol{L}^2(\Omega_1)}^2 \to 0.
\end{aligned}$$

This proves the result for $\boldsymbol{L}^2(\Omega_\tau)$. From the uniqueness of weak limits and the continuous inclusion $L^2(\boldsymbol{H}^1) \subseteq L^2(\Omega_\tau)$, we thus even conclude the result for $\boldsymbol{L}^2(\boldsymbol{H}^1)$.

□

The remainder of this section is dedicated to proving the second part of our main result. We start by identifying the limit function $\boldsymbol{v}$.

Lemma 12. *It holds $\boldsymbol{v} = \boldsymbol{m}_\tau$ almost everywhere in Ω_τ.*

Proof. The proof is technical but straightforward and we therefore only sketch it. Using the fact that

$$\left|\frac{\boldsymbol{m}_h^{j+1} - \boldsymbol{m}_h^j}{k} - \boldsymbol{v}_h^j\right| \leq \frac{1}{2}k|\boldsymbol{v}_h^j|^2, \tag{37}$$

we proceed as in [1, 14] to see that

$$\|\partial_\tau \boldsymbol{m}_{hk} - \boldsymbol{v}_{hk}\|_{\boldsymbol{L}^1(\Omega_\tau)} \lesssim k\|\boldsymbol{v}_{hk}\|^2_{\boldsymbol{L}^2(\Omega_\tau)}.$$

Exploiting weak semi-continuity of $\|\cdot\|_{\boldsymbol{L}^1(\Omega_\tau)}$, this yields

$$\|\boldsymbol{m}_\tau - \boldsymbol{v}\|_{\boldsymbol{L}^1(\Omega_\tau)} \leq \liminf \|\partial_\tau \boldsymbol{m}_{hk} - \boldsymbol{v}_{hk}\|_{\boldsymbol{L}^1(\Omega_\tau)} = 0$$

and thus the desired result. $\square$

With these results, we can finally prove our main theorem.

Proof of Theorem 7 (b). Let $\boldsymbol{\phi} \in C^\infty(\Omega_\tau)$ be arbitrary. We define test functions by $\boldsymbol{\phi}_h(t,\cdot) := \big(\mathcal{I}_h(\boldsymbol{m}_{hk}^- \times \boldsymbol{\phi})\big)(t,\cdot)$. From (26) we thus get

$$\begin{aligned}\alpha \int_0^{\tau_\text{end}} \langle \boldsymbol{v}_{hk}^-, \boldsymbol{\phi}_h\rangle + C_\text{exch} k\theta \int_0^{\tau_\text{end}} \langle \nabla \boldsymbol{v}_{hk}^-, \nabla \boldsymbol{\phi}_h\rangle + \int_0^{\tau_\text{end}} \Big\langle (\boldsymbol{m}_{hk}^- \times \boldsymbol{v}_{hk}^-), \boldsymbol{\phi}_h\Big\rangle \\ = -C_\text{exch} \int_0^{\tau_\text{end}} \langle \nabla \boldsymbol{m}_{hk}^-, \nabla \boldsymbol{\phi}_h\rangle - \int_0^{\tau_\text{end}} \Big\langle \boldsymbol{\pi}_h(\boldsymbol{m}_{hk}^-, \zeta_{hk}^-), \boldsymbol{\phi}_h\Big\rangle + \int_0^t \langle \boldsymbol{f}_{hk}^-, \boldsymbol{\phi}_h\rangle.\end{aligned}$$

Exploiting the shape of $\boldsymbol{\phi}_h$ and using the approximation properties of the nodal interpolation operator $\mathcal{I}_h$, we get

$$\begin{aligned}\int_0^T \Big\langle (\alpha \boldsymbol{v}_{hk}^- + \boldsymbol{m}_{hk}^- \times \boldsymbol{v}_{hk}^-), (\boldsymbol{m}_{hk}^- \times \boldsymbol{\phi})\Big\rangle + C_\text{exch} k\theta \int_0^{\tau_\text{end}} \Big\langle \nabla \boldsymbol{v}_{hk}^-, \nabla(\boldsymbol{m}_{hk}^- \times \boldsymbol{\phi})\Big\rangle \\ + C_\text{exch} \int_0^{\tau_\text{end}} \Big\langle \nabla \boldsymbol{m}_{hk}^-, \nabla(\boldsymbol{m}_{hk}^- \times \boldsymbol{\phi})\Big\rangle \\ + \int_0^{\tau_\text{end}} \Big\langle \boldsymbol{\pi}_h(\boldsymbol{m}_{hk}^-, \zeta_{hk}^-), (\boldsymbol{m}_{hk}^- \times \boldsymbol{\phi})\Big\rangle \\ - \int_0^{\tau_\text{end}} \Big\langle \boldsymbol{f}_{hk}^-, (\boldsymbol{m}_{hk}^- \times \boldsymbol{\phi})\Big\rangle \\ = \mathcal{O}(h).\end{aligned}$$

Next, we proceed as in [1, 14] to see that

$$\begin{aligned}\int_0^{\tau_\text{end}} \Big\langle (\alpha \boldsymbol{v}_{hk}^- + \boldsymbol{m}_{hk}^- \times \boldsymbol{v}_{hk}^-), (\boldsymbol{m}_{hk}^- \times \boldsymbol{\phi})\Big\rangle \longrightarrow \int_0^{\tau_\text{end}} \Big\langle (\alpha \boldsymbol{m}_t + \boldsymbol{m} \times \boldsymbol{m}_t), (\boldsymbol{m} \times \boldsymbol{\phi})\Big\rangle, \\ k\,\theta \int_0^{\tau_\text{end}} \Big\langle \nabla \boldsymbol{v}_{hk}^-, \nabla(\boldsymbol{m}_{hk}^- \times \boldsymbol{\phi})\Big\rangle \longrightarrow 0, \quad \text{and} \\ \int_0^{\tau_\text{end}} \Big\langle \nabla \boldsymbol{m}_{hk}^-, \nabla(\boldsymbol{m}_{hk}^- \times \boldsymbol{\phi})\Big\rangle \longrightarrow \int_0^{\tau_\text{end}} \Big\langle \nabla \boldsymbol{m}, \nabla(\boldsymbol{m} \times \boldsymbol{\phi})\Big\rangle.\end{aligned} \tag{38}$$

Here, we have used the boundedness of $\sqrt{k}\|\nabla \boldsymbol{v}_{hk}^-\|_{\boldsymbol{L}^2(\Omega_\tau)}$, which follows from (33) for $j = N$, and thus $\theta \in (1/2, 1]$. From the convergence $(\boldsymbol{m}_{hk}^- \times \boldsymbol{\phi}) \to (\boldsymbol{m} \times \boldsymbol{\phi})$ strongly in

$\boldsymbol{L}^2(\Omega_\tau)$ and the assumptions (30) and (32) on $\boldsymbol{f}_{hk}^-$ and $\boldsymbol{\pi}_h(\boldsymbol{m}_{hk}^-,\zeta_{hk}^-)$, we conclude

$$\int_0^{\tau_{\text{end}}} \Big\langle \boldsymbol{\pi}_h(\boldsymbol{m}_{hk}^-,\zeta_{hk}^-),(\boldsymbol{m}_{hk}^-\times\boldsymbol{\phi})\Big\rangle \longrightarrow \int_0^{\tau_{\text{end}}} \Big\langle \boldsymbol{\pi}(\boldsymbol{m},\zeta),(\boldsymbol{m}\times\boldsymbol{\phi})\Big\rangle, \qquad \text{and}$$
$$\int_0^{\tau_{\text{end}}} \Big\langle \boldsymbol{f}_{hk}^-,(\boldsymbol{m}_{hk}^-\times\boldsymbol{\phi})\Big\rangle \longrightarrow \int_0^{\tau_{\text{end}}} \Big\langle \boldsymbol{f},(\boldsymbol{m}\times\boldsymbol{\phi})\Big\rangle.$$

Altogether we have now shown

$$\begin{aligned}\alpha\int_0^{\tau_{\text{end}}} \Big\langle \boldsymbol{m}_t,(\boldsymbol{m}\times\boldsymbol{\phi})\Big\rangle + \int_0^{\tau_{\text{end}}} \Big\langle (\boldsymbol{m}\times\boldsymbol{m}_t),(\boldsymbol{m}\times\boldsymbol{\phi})\Big\rangle &= -C_{\text{exch}}\int_0^{\tau_{\text{end}}} \Big\langle \nabla\boldsymbol{m},\nabla(\boldsymbol{m}\times\boldsymbol{\phi})\Big\rangle \\ &\quad - \int_0^{\tau_{\text{end}}} \Big\langle \boldsymbol{\pi}(\boldsymbol{m},\zeta),(\boldsymbol{m}\times\boldsymbol{\phi})\Big\rangle \\ &\quad + \int_0^{\tau_{\text{end}}} \Big\langle \boldsymbol{f},(\boldsymbol{m}\times\boldsymbol{\phi})\Big\rangle.\end{aligned}$$

Using the identities

$$\begin{aligned}(\boldsymbol{m}\times\boldsymbol{m}_t)\cdot(\boldsymbol{m}\times\boldsymbol{\phi}) &= \boldsymbol{m}_t\cdot\boldsymbol{\phi}, \\ \nabla\boldsymbol{m}\cdot\nabla(\boldsymbol{m}\times\boldsymbol{\phi}) &= \nabla\boldsymbol{m}\cdot(\boldsymbol{m}\times\nabla\boldsymbol{\phi}),\end{aligned}$$

as well as the property $a\cdot(b\times c)=(a\times b)\cdot c$ of the cross product, we conclude (21). It remains to show the energy estimate (22) and the modulus constraint of $\boldsymbol{m}$. From the discrete energy estimate (33), we get for any $t'\in[0,\tau_{\text{end}}]$ with $t'\in[\tau_j,\tau_{j+1})$

$$\begin{aligned}\|\nabla\boldsymbol{m}_{hk}^+(t')\|_{L^2(\Omega_1)}^2 + C_1\|\boldsymbol{v}_{hk}^-\|_{L^2(\Omega_{t'})}^2 &= \|\nabla\boldsymbol{m}_{hk}^+(t')\|_{L^2(\Omega_1)}^2 + C_1\int_0^{t'}\|\boldsymbol{v}_{hk}^-(t)\|_{L^2(\Omega_1)}^2 \\ &\le \|\nabla\boldsymbol{m}_{hk}^+(t')\|_{L^2(\Omega_1)}^2 + C_1\int_0^{\tau_{j+1}}\|\boldsymbol{v}_{hk}^-(t)\|_{L^2(\Omega_1)}^2 \\ &= \|\nabla\boldsymbol{m}_{hk}^+(t')\|_{L^2(\Omega_1)}^2 + C_1 k\sum_{i=0}^{j}\|\boldsymbol{v}_h^i\|_{L^2(\Omega_1)}^2 \\ &\le \|\nabla\boldsymbol{m}_h^0\|_{L^2(\Omega_1)}^2 + C_2.\end{aligned}$$

Integration in time thus yields for any Borel set $\mathfrak{T}\in[0,\tau_{\text{end}}]$

$$\int_{\mathfrak{T}}\|\nabla\boldsymbol{m}_{hk}^+(t')\|_{L^2(\Omega_1)}^2 + C_1\int_{\mathfrak{T}}\|\boldsymbol{v}_{hk}^-\|_{L^2(\Omega_{t'})}^2 \le \int_{\mathfrak{T}}\|\nabla\boldsymbol{m}_h^0\|_{L^2(\Omega_1)}^2 + \int_{\mathfrak{T}} C_2.$$

Hence, weak semi-continuity of $\int_{\mathfrak{T}}\|\cdot\|_{\boldsymbol{L}^2(\Omega_1)}^2$ leads to

$$\int_{\mathfrak{T}}\|\nabla\boldsymbol{m}\|_{L^2(\Omega_1)}^2 + C_1\int_{\mathfrak{T}}\|\boldsymbol{m}_\tau\|_{L^2(\Omega_{t'})}^2 \le \int_{\mathfrak{T}}\|\nabla\boldsymbol{m}^0\|_{L^2(\Omega_1)}^2 + \int_{\mathfrak{T}} C_2.$$

From

$$\||\boldsymbol{m}|-1\|_{\boldsymbol{L}^2(\Omega_\tau)} \le \||\boldsymbol{m}|-|\boldsymbol{m}_{hk}^-|\|_{\boldsymbol{L}^2(\Omega_\tau)} + \||\boldsymbol{m}_{hk}^-|-1\|_{\boldsymbol{L}^2(\Omega_\tau)}$$

and

$$\||\boldsymbol{m}_{hk}^-(t,\cdot)|-1\|_{\boldsymbol{L}^2(\Omega_1)} \le h\max_{\tau_j}\|\nabla\boldsymbol{m}_h^j\|_{\boldsymbol{L}^2(\Omega_1)},$$

we finally deduce $|\boldsymbol{m}|=1$ almost everywhere in Ω_τ. The equality $\boldsymbol{m}(0,\cdot)=\boldsymbol{m}^0$ in the trace sense follows from weak $\boldsymbol{H}^1(\Omega_\tau)$ convergence of $\boldsymbol{m}_{hk}$ and thus weak convergence of the traces. Using the weak convergence $\boldsymbol{m}_h^0\rightharpoonup\boldsymbol{m}^0$ identifies the sought limit. This concludes the proof. $\square$

Remark 13. *Note that in case of the Crank-Nicholson scheme ($\theta=1/2$) one needs an additional bound for $\nabla\boldsymbol{v}_{hk}^-$ in* (38)*. As in* [1, 2], [14] *this can be done by using an inverse estimate. In this case, however, we end up with a (weak) coupling of h and k but can still proof convergence as long as k/h tends to* 0.

4. Effective Field Contributions for Multiscale LLG Equation

In this section, we aim to give examples for contributions $\boldsymbol{\pi}$ and corresponding discretizations $\boldsymbol{\pi}_h$ which guarantee the assumptions (31)–(32) of our main result in Theorem 7. In particular, we will see that the contributions of our multiscale LLG model satisfy these assumptions.

4.1. **Function spaces.** Let $\mathcal{T}_h^{\Omega_j}$ denote a conforming triangulation of Ω_j $(j = 1, 2)$ into compact and non-degenerate tetrahedra $T \in \mathcal{T}_h^{\Omega_j}$. Let $H^1_*(\Omega_j)$ be the Hilbert space of all functions $v \in H^1(\Omega_j)$ satisfying $\int_{\Omega_j} v\,dx = 0$ and let $H^1_0(\Omega_j)$ be the Hilbert space of all functions $v \in H^1(\Omega_j)$ with $v^{\mathrm{int}} = 0$ on Γ_j, where $\Gamma_j = \partial\Omega_j$ denotes the corresponding boundary. By $H(\mathrm{div}\,, \Omega_j)$ we denote those functions on Ω_j whose divergence is in $\boldsymbol{L}^2(\Omega_j)$. We define the discrete function spaces $\mathcal{S}^1_*(\mathcal{T}_h^{\Omega_j}) \subseteq H^1_*(\Omega_j)$ resp. $\mathcal{S}^1_0(\mathcal{T}_h^{\Omega_j}) \subseteq H^1_0(\Omega_j)$ by $\mathcal{S}^1_*(\mathcal{T}_h^{\Omega_j}) = H^1_*(\Omega_j) \cap \mathcal{S}^1(\mathcal{T}_h^{\Omega_j})$ resp. $\mathcal{S}^1_0(\mathcal{T}_h^{\Omega_j}) = H^1_0(\Omega_j) \cap \mathcal{S}^1(\mathcal{T}_h^{\Omega_j})$, where, analogously to (23), $\mathcal{S}^1(\mathcal{T}_h^{\Omega_j})$ denotes the space of piecewise affine and globally continuous functions on $\mathcal{T}_h^{\Omega_j}$. The triangulation $\mathcal{T}_h^{\Omega_j}$ induces a conforming triangulation of the boundary $\mathcal{E}_h^{\Gamma_j} := \mathcal{T}_h^{\Omega_j}|_{\Gamma_j}$. Additionally, we define the discrete space $\mathcal{P}^0(\mathcal{E}_h^{\Gamma_j}) = \Big\{\psi \,:\, \psi|_E \text{ constant for all } E \in \mathcal{E}_h^{\Gamma_j}\Big\}$ of all piecewise constant functions on the boundary.

4.2. **Pointwise operators and anisotropy energy contribution.** With $\mathbb{B} := \Big\{x \in \mathbb{R}^3 \,:\, |x| \le 1\Big\}$ the compact unit ball in $\mathbb{R}^3$, let $\phi : \mathbb{B} \to \mathbb{R}$ be a Lipschitz continuous anisotropy density. Possible examples include the uniaxial density $\phi(x) = -\frac{1}{2}\,(x \cdot \boldsymbol{e})^2$ with a given easy axis $\boldsymbol{e} \in \mathbb{S} := \Big\{x \in \mathbb{R}^3 \,:\, |x| = 1\Big\}$ as well as the cubic density $\phi(x) = K_1(x_1^2x_2^2 + x_2^2x_3^2) + K_2x_1^2x_2^2x_3^2$ with certain constants $K_1, K_2 \ge 0$. According to Rademacher's theorem, ϕ is differentiable pointwise almost everywhere with $D\phi \in \boldsymbol{L}^\infty(\mathbb{B})$. Therefore, the anisotropy contribution to the effective field reads

$$\Big(\boldsymbol{\pi}(\boldsymbol{n}, \zeta)\Big)(x) = \Big(\boldsymbol{\pi}(\boldsymbol{n})\Big)(x) = D\phi\Big(\boldsymbol{n}(x)\Big) \quad \text{for } \boldsymbol{n} \in \boldsymbol{L}^2(\Omega_1) \text{ and almost all } x \in \Omega_1, \tag{39}$$

and $\boldsymbol{\pi}_h(\cdot) = \boldsymbol{\pi}(\cdot)$. Note that in this case, we neglected a possible dependence on ζ, i.e. formally $Y = \{0\}$ and ζ_{hk}^- denotes the constant zero sequence.

Proposition 14. *Suppose that $\boldsymbol{\Phi} \in \boldsymbol{L}^\infty(\mathbb{B})$, e.g. $\boldsymbol{\Phi}(x) = D\phi(x)$, and $\boldsymbol{\pi}_h(\boldsymbol{n}) := \boldsymbol{\pi}(\boldsymbol{n}) := \boldsymbol{\Phi} \circ \boldsymbol{n}$. Then, the assumptions* (31)–(32) *of Theorem 7 are satisfied.*

Proof. Clearly, (31) holds with $C_1 = \|\boldsymbol{\Phi}\|_{\boldsymbol{L}^\infty(\Omega_1)}$. Part (a) of Theorem 7 thus predicts strong subconvergence $\boldsymbol{m}_{hk}^- \to \boldsymbol{m}$ in $\boldsymbol{L}^2(\Omega_\tau)$. Now, choose sequences $h_\ell \to 0$, $k_\ell \to 0$ such that $\boldsymbol{m}_\ell := \boldsymbol{m}_{h_\ell k_\ell}^-$ converges strongly in $\boldsymbol{L}^2(\Omega_\tau)$ to $\boldsymbol{m}$. By extracting a subsequence, we may in particular assume that $\boldsymbol{m}_\ell$ converges to $\boldsymbol{m}$ even pointwise almost everywhere in Ω_τ. This implies $\boldsymbol{\pi}(\boldsymbol{m}_\ell) \to \boldsymbol{\pi}(\boldsymbol{m})$ pointwise almost everywhere in Ω_τ. In particular, $|\boldsymbol{m}_\ell| \le 1$ also implies $|\boldsymbol{m}| \le 1$ almost everywhere. Moreover and because of (31), $|\boldsymbol{\pi}(\boldsymbol{m}) - \boldsymbol{\pi}(\boldsymbol{m}_\ell)| \le 2C_1$ is uniformly bounded in $\boldsymbol{L}^\infty(\Omega_\tau)$. Finally, the Lebesgue dominated convergence theorem thus applies and proves even strong convergence of $\boldsymbol{\pi}(\boldsymbol{m}_\ell)$ to $\boldsymbol{\pi}(\boldsymbol{m})$ in $\boldsymbol{L}^2(\Omega_\tau)$. $\square$

4.3. **Uniformly monotone operators.** We consider the frame of the Browder-Minty theorem, see [29, Section 26.2]: Let X be a separable Hilbert space, $A : X \to X^*$ be a uniformly monotone, coercive, and hemicontinuous (nonlinear) operator, and $b \in X^*$. Under these assumptions, the Browder-Minty theorem states that the operator equation

$$Aw = b \tag{40}$$

has a unique solution $w \in X$. Arguing as in the original proof, one has the following: For $h > 0$, let $X_h \subseteq X$ be finite dimensional subspaces of X with $X_h \subseteq X_{h'}$ for $h > h'$ and $\overline{\bigcup_{h>0} X_h} = X$. Let $b_h \in X_h^*$. Then, the Galerkin formulation

$$\langle Aw_h, v_h \rangle_{X_h^* \times X_h} = \langle b_h, v_h \rangle_{X_h^* \times X_h} \quad \text{for all } v_h \in X_h \tag{41}$$

admits a unique solution $w_h \in X_h$. Provided $\|b_h\|_{X_h^*} \le M < \infty$ for all $h > 0$, the sequence of Galerkin solutions is bounded, i.e. $\|w_h\|_{X_h} \le C < \infty$ for all $h > 0$, and the h-independent constant $C > 0$ depends only on M and the coercivity of A. In particular, the sequence (w_h) is weakly subconvergent in X towards some limit $w \in X$. If $\lim_{h\to 0} \|b - b_h\|_{X_h^*} = 0$, this limit solves the operator equation (40). Finally, uniform monotonicity implies that there even holds strong convergence $\lim_{h\to 0} \|w - w_h\|_X = 0$ of the entire sequence.

This framework is now used in the following lemma which guarantees the assumptions (31)–(32) of Theorem 7 for certain energy contributions:

Lemma 15. *Let Y be a Banach space and let $S, S_h \in L\Big(X, \boldsymbol{L}^2(\Omega_1)\Big)$, and $T, T_h \in L\Big(\boldsymbol{L}^2(\Omega_1) \times Y, X^*\Big)$ with*

$$S_h x \rightharpoonup Sx \quad \text{weakly in } \boldsymbol{L}^2(\Omega_1) \text{ for all } x \in X, \tag{42}$$

$$T_h(\boldsymbol{n}, y) \to T(\boldsymbol{n}, y) \quad \text{strongly in } X^* \text{ for all } \boldsymbol{n} \in \boldsymbol{L}^2(\Omega_1), y \in Y, \tag{43}$$

and $\boldsymbol{\pi}(\cdot) := SA^{-1}T : \boldsymbol{L}^2(\Omega_1) \times Y \to \boldsymbol{L}^2(\Omega_1)$. For $h > 0$, $\boldsymbol{n} \in \boldsymbol{L}^2(\Omega_1)$, and $y \in Y$, define the approximate operator $\boldsymbol{\pi}_h(\boldsymbol{n}, y) := S_h u_h$, where u_h is the unique Galerkin solution of

$$\langle Au_h, v_h \rangle_{X_h^* \times X_h} = \langle T_h(\boldsymbol{n}, y), v_h \rangle_{X_h^* \times X_h} \quad \text{for all } v_h \in X_h. \tag{44}$$

Under the foregoing assumptions, it holds that

$$\|\boldsymbol{\pi}_h(\boldsymbol{n}, y)\|_{\boldsymbol{L}^2(\Omega_1)} \le C_4 \tag{45}$$

for all $\boldsymbol{n} \in \boldsymbol{L}^2(\Omega_1)$ with $|\boldsymbol{n}| \le 1$ almost everywhere and all $y \in Y$ with $\|y\|_Y \le C_3$ for some constant $C_3 > 0$, and for all $h > 0$. The constant $C_4 > 0$ does not depend on y and $\boldsymbol{n}$, but only on Ω and C_3. Moreover, strong subconvergence $(\boldsymbol{m}_{hk}^-, \zeta_{hk}^-) \to (\boldsymbol{m}, \zeta)$ in $\boldsymbol{L}^2\Big([0,\tau]; (\boldsymbol{L}^2(\Omega_1) \times Y)\Big) = L^2(\boldsymbol{L}^2(\Omega_1) \times Y)$ for some sequence $\zeta_{hk}^- \in L^\infty(Y)$ implies weak subconvergence $\boldsymbol{\pi}_h(\boldsymbol{m}_{hk}^-, \zeta_{hk}^-) \rightharpoonup \boldsymbol{\pi}(\boldsymbol{m}, \zeta)$ in $\boldsymbol{L}^2(\Omega_\tau)$ as $(h,k) \to (0,0)$.

Proof. The Banach-Steinhaus theorem implies uniform boundedness $C_S := \sup_{h>0} \|S_h\| < \infty$ and $C_T := \sup_{h>0} \|T_h\| < \infty$ of the respective operator norms. For fixed $\boldsymbol{n} \in \boldsymbol{L}^2(\Omega_1)$ with $|\boldsymbol{n}| \le 1$ almost everywhere, $y \in Y$ with $\|y\|_Y \le C_3$, and $b_h := T_h(\boldsymbol{n}, y)$, this implies

$$\|b_h\|_{\boldsymbol{L}^2(\Omega_1)} \le C_T \|(\boldsymbol{n}, y)\|_{\boldsymbol{L}^2(\Omega_1) \times Y} \le C_T \Big(|\Omega_1| + C_3^2\Big)^{1/2} =: M < \infty.$$

Thus, we infer $\|u_h\|_X \le C < \infty$, where $C > 0$ does neither depend on h nor on $(\boldsymbol{n}, y)$, but only on M. Consequently, this proves (45) with $C_4 = CC_S$.

Next, we aim to show that $\boldsymbol{\pi}_h(\boldsymbol{n}_h, y_h) \rightharpoonup \boldsymbol{\pi}_h(\boldsymbol{n}, y)$ weakly in $\boldsymbol{L}^2(\Omega_1)$ as $h \to 0$ provided that $(\boldsymbol{n}_h, y_h) \to (\boldsymbol{n}, y)$ strongly in $\boldsymbol{L}^2(\Omega_1) \times Y$. By assumption (43) on T_h, we have $T_h(\boldsymbol{n}, y) \to T(\boldsymbol{n}, y)$ strongly in X^* as $h \to 0$. Together with uniform boundedness of T_h, this implies $T_h(\boldsymbol{n}_h, y_h) = T_h(\boldsymbol{n}, y) - T_h\Big((\boldsymbol{n} - \boldsymbol{n}_h, y - y_h)\Big) \to T(\boldsymbol{n}, y)$ strongly in X^* as $h \to 0$. Therefore, the Browder-Minty theorem for uniformly monotone operators guarantees $u_h \to u$ strongly in X, where $u = A^{-1}T(\boldsymbol{n}, y)$ and $u_h \in X_h$ solves (44) with $(\boldsymbol{n}, y)$ replaced by $(\boldsymbol{n}_h, y_h)$. The convergence assumption (42) and the uniform boundedness of S_h thus show $\boldsymbol{\pi}_h(\boldsymbol{n}_h, y_h) = S_h u_h = S_h u - S_h(u - u_h) \rightharpoonup Su = \boldsymbol{\pi}(\boldsymbol{n}, y)$ weakly in $\boldsymbol{L}^2(\Omega_1)$ as $h \to 0$.

Finally, we prove weak subconvergence $\boldsymbol{\pi}_h(\boldsymbol{m}_{hk}^-, \zeta_{hk}^-) \rightharpoonup \boldsymbol{\pi}(\boldsymbol{m}, \zeta)$ in $\boldsymbol{L}^2(\Omega_\tau)$ as $(h, k) \to (0, 0)$. To that end, we choose sequences $h_\ell \to 0$, $k_\ell \to 0$ such that $(\boldsymbol{m}_\ell, \zeta_\ell) := (\boldsymbol{m}_{h_\ell k_\ell}^-, \zeta_{h_\ell k_\ell}^-)$ converges strongly in $L^2\Big(\boldsymbol{L}^2(\Omega_1) \times Y\Big)$ to $(\boldsymbol{m}, \zeta)$. By extracting a further subsequence, we may assume that $\boldsymbol{m}_\ell(t) \to \boldsymbol{m}(t)$ strongly in $\boldsymbol{L}^2(\Omega_1)$ as well as $\zeta_\ell(t) \to \zeta(t)$ in Y, for almost all times t. Define $\boldsymbol{\pi}_\ell := \boldsymbol{\pi}_{h_\ell}$ and let $\boldsymbol{\phi} \in \boldsymbol{L}^2(\Omega_\tau)$. Then,

$$\Big(\boldsymbol{\pi}_\ell\Big((\boldsymbol{m}_\ell, \zeta_\ell)\Big) - \boldsymbol{\pi}\Big((\boldsymbol{m}, \zeta)\Big), \boldsymbol{\phi}\Big) = \int_0^{\tau_{\mathrm{end}}} \langle \boldsymbol{\pi}_\ell\Big((\boldsymbol{m}_\ell(t), \zeta_\ell(t))\Big) - \boldsymbol{\pi}\Big((\boldsymbol{m}(t), \zeta(t)\Big), \boldsymbol{\phi}(t)\rangle \, dt.$$

From weak convergence $\boldsymbol{\pi}_\ell\Big((\boldsymbol{m}_\ell(t), \zeta_\ell(t))\Big) \rightharpoonup \boldsymbol{\pi}\Big((\boldsymbol{m}(t), \zeta(t))\Big)$ as $\ell \to \infty$ for almost all times t, we see pointwise convergence of the integrand to zero. According to (45) and the assumption $\zeta_{hk}^- \in \boldsymbol{L}^\infty(Y)$, the Lebesgue dominated convergence theorem thus proves

$$\Big(\boldsymbol{\pi}_\ell\Big((\boldsymbol{m}_\ell, \zeta_\ell)\Big) - \boldsymbol{\pi}\Big((\boldsymbol{m}, \zeta)\Big), \boldsymbol{\phi}\Big) \to 0 \quad \text{as } \ell \to \infty.$$

This concludes the proof. □

Remark 16. (i) *Similar arguments as in the proof of Lemma 15 reveal that strong convergence $S_h x \to Sx$ in* (42) *also results in strong convergence $\boldsymbol{\pi}_h(\boldsymbol{m}_{hk}^-, \zeta_{hk}^-) \to \boldsymbol{\pi}(\boldsymbol{m}, \zeta)$ in $\boldsymbol{L}^2(\Omega_\tau)$ as $h, k \to 0$.*
(ii) *The abstract framework applies, in particular, to linear contributions $\boldsymbol{\pi}_h(\cdot) = S_h$ of the effective field $\boldsymbol{h}_{\mathrm{eff}}$, where $X = \boldsymbol{L}^2(\Omega_1)$, $Y = \{0\}$, and the operators $A = A_h$ as well as $T = T_h$ are just the identities. In this case, $\zeta_{hk}^- = 0$ for all $(h, k) > 0$. In particular, we may therefore write $\boldsymbol{\pi}_h(\boldsymbol{m}_{hk}^-, \zeta_{hk}^-) = \boldsymbol{\pi}_h(\boldsymbol{m}_{hk}^-)$.*
(iii) *For the multiscale approach, we use $Y = \boldsymbol{H}(\mathrm{div}\,; \Omega_2)$, $\zeta_{hk}^- = \boldsymbol{f}_{hk}^-$, and $\zeta = \boldsymbol{f}$, respectively.*

4.4. **Integral operators and mapping properties.** The following applications need two integral operators for either Γ_i, namely the double-layer potential $\widetilde{K}_i$ and the simple-layer potential $\widetilde{V}_i$, which formally read

$$(\widetilde{K}_i v)(x) = \frac{1}{4\pi} \int_{\Gamma_i} \frac{(x - y) \cdot \boldsymbol{\nu}(y)}{|x - y|^3} v(y) \, d\Gamma(y), \tag{46}$$

$$(\widetilde{V}_i \phi)(x) = \frac{1}{4\pi} \int_{\Gamma_i} \frac{1}{|x - y|} \phi(y) \, d\Gamma(y), \tag{47}$$

for all $x \in \mathbb{R}^3 \backslash \Gamma_i$. These operators may be extended to bounded, linear operators $\widetilde{K}_i : H^{1/2}(\Gamma_i) \to H^1(\mathbb{R}^3 \backslash \Gamma_i)$ and $\widetilde{V}_i : H^{-1/2}(\Gamma_i) \to H^1(\mathbb{R}^3)$, see e.g. [18, 21, 24]. There holds

$$\Delta \widetilde{K}_i v = \Delta \widetilde{V}_i \phi = 0 \quad \text{on } \mathbb{R}^3 \backslash \Gamma_i \quad \text{and} \quad \widetilde{K}_i v, \widetilde{V}_i \phi \in C^\infty(\mathbb{R}^3 \backslash \Gamma_i). \tag{48}$$

Via restriction to the boundary Γ_i, one obtains

$$(\widetilde{K}_i v)^{\mathrm{int}} = (K_i - 1/2) v \quad \text{and} \quad (\widetilde{V}_i \phi)^{\mathrm{int}} = V_i \phi, \tag{49}$$

where the operators $K_i : H^{1/2}(\Gamma_i) \to H^{1/2}(\Gamma_i)$ and $V_i : H^{-1/2}(\Gamma_i) \to H^{1/2}(\Gamma_i)$ coincide formally with $\widetilde{K}_i$ and $\widetilde{V}_i$, but are evaluated on the boundary Γ_i. There hold the following jump properties across the boundary Γ_i, cf. e.g. [24, Theorem 3.3.1]:

$$(\widetilde{K}_i v)^{\mathrm{ext}} - (\widetilde{K}_i v)^{\mathrm{int}} = v, \qquad \partial_{\boldsymbol{\nu}}^{\mathrm{ext}} \widetilde{K}_i v - \partial_{\boldsymbol{\nu}}^{\mathrm{int}} \widetilde{K}_i v = 0, \tag{50}$$

$$(\widetilde{V}_i \phi)^{\mathrm{ext}} - (\widetilde{V}_i \phi)^{\mathrm{int}} = 0, \qquad \partial_{\boldsymbol{\nu}}^{\mathrm{ext}} \widetilde{V}_i \phi - \partial_{\boldsymbol{\nu}}^{\mathrm{int}} \widetilde{V}_i \phi = -\phi. \tag{51}$$

4.5. **Application: Hybrid FEM-BEM approach for strayfield contribution.** In the following, we present the approach of FREDKIN and KOEHLER, see [10], for the approximate computation of the strayfield contribution and show that it satisfies the desired properties to apply Lemma 15.

4.5.1. *Continuous formulation of Fredkin-Koehler approach.* Given any $\boldsymbol{m} \in L^2(\Omega_1)$, the non-dimensional form of (9) reads

$$\begin{array}{rcll} \Delta u_1 &=& \nabla \cdot \boldsymbol{m} & \text{in } \Omega_1, \\ \Delta u_1 &=& 0 & \text{in } \mathbb{R}^3 \backslash \overline{\Omega}_1, \\ u_1^{\text{ext}} - u_1^{\text{int}} &=& 0 & \text{on } \Gamma_1, \\ \partial_{\boldsymbol{\nu}} u_1^{\text{ext}} - \partial_{\boldsymbol{\nu}} u_1^{\text{int}} &=& -\boldsymbol{m} \cdot \boldsymbol{\nu} & \text{on } \Gamma_1, \\ u_1(x) &=& \mathcal{O}(1/|x|) & \text{as } |x| \to \infty. \end{array} \tag{52}$$

In a first step, let $u_{11} \in H^1_*(\Omega_1)$ be the unique solution of the Neumann problem

$$\begin{array}{rcll} \Delta u_{11} &=& \nabla \cdot \boldsymbol{m} & \text{in } \Omega_1, \\ \partial_{\boldsymbol{\nu}} u_{11} &=& \boldsymbol{m} \cdot \boldsymbol{\nu} & \text{on } \Gamma_1. \end{array} \tag{53}$$

Next, consider u_{11} extended by zero to the entire space $\mathbb{R}^3 \backslash \overline{\Omega}_1$. The remainder $u_{12} = u_1 - u_{11}$ satisfies

$$\begin{array}{rcll} \Delta u_{12} &=& 0 & \text{in } \Omega_1, \\ \Delta u_{12} &=& 0 & \text{in } \mathbb{R}^3 \backslash \overline{\Omega}_1, \\ u_{12}^{\text{ext}} - u_{12}^{\text{int}} &=& u_{11}^{\text{int}} & \text{on } \Gamma_1, \\ \partial_{\boldsymbol{\nu}} u_{12}^{\text{ext}} - \partial_{\boldsymbol{\nu}} u_{12}^{\text{int}} &=& 0 & \text{on } \Gamma_1, \\ u_{12}(x) &=& \mathcal{O}(1/|x|) & \text{as } |x| \to \infty. \end{array} \tag{54}$$

The unique solution $u_{12} \in H^1(\mathbb{R}^3 \backslash \Gamma_1)$ of the transmission problem (54) is the double-layer potential

$$u_{12}(x) = (\widetilde{K}_1 u_{11}^{\text{int}})(x). \tag{55}$$

Due to harmonicity of $\widetilde{K}_1 u_{11}^{\text{int}}$ in Ω_1, see (48) and the definition of K_1 in (49), u_{12} is characterized by the inhomogeneous Dirichlet problem

$$\begin{array}{rcll} \Delta u_{12} &=& 0 & \text{in } \Omega_1, \\ u_{12}^{\text{int}} &=& (K_1 - 1/2) u_{11}^{\text{int}} & \text{on } \Gamma_1, \end{array} \tag{56}$$

and we have $u_1 = u_{11} + u_{12}$ and hence $\nabla u_1 = \nabla u_{11} + \nabla u_{12}$ in Ω_1.

4.5.2. *Discrete formulation and convergence analysis.* To discretize the equations (53) and (56), we use lowest-order Courant finite elements: First, let $u_{11h} \in \mathcal{S}^1_*(\mathcal{T}_h^{\Omega_1})$ be the unique FE solution of

$$\int_{\Omega_1} \nabla u_{11h} \cdot \nabla v_h \, dx = \int_{\Omega_1} \boldsymbol{m} \cdot \nabla v_h \, dx \quad \text{for all } v_h \in \mathcal{S}^1_*(\mathcal{T}_h^{\Omega_1}). \tag{57}$$

Since an FE solution $u_{12h} \in \mathcal{S}^1(\mathcal{T}_h^{\Omega_1})$ of (56) cannot satisfy continuous Dirichlet data $(K_1 - 1/2) u_{11h}^{\text{int}}$, we need to discretize the Dirichlet data. To that end, let $I_h^{\Omega_1} : H^1(\Omega_1) \to \mathcal{S}^1(\mathcal{T}_h^{\Omega_1})$ be the Scott-Zhang projection from [26]. Since $I_h^{\Omega_1}$ is H^1-stable and preserves discrete boundary data, it induces a stable projection $I_h^{\Gamma_1} : H^{1/2}(\Gamma_1) \to \mathcal{S}^1(\mathcal{T}_h^{\Omega_1}|_{\Gamma_1})$ with $(I_h^{\Omega_1} v)^{\text{int}} = I_h^{\Gamma_1}(v^{\text{int}})$ for all $v \in H^1(\Omega_1)$. Then, we let $u_{12h} \in \mathcal{S}^1(\mathcal{T}_h^{\Omega_1})$ with $u_{12h}^{\text{int}} = I_h^{\Gamma_1}(K_1 - 1/2) u_{11h}^{\text{int}}$ be the unique solution of the inhomogeneous Dirichlet problem

$$\int_{\Omega_1} \nabla u_{12h} \cdot \nabla v_h \, dx = 0 \quad \text{for all } v_h \in \mathcal{S}^1_0(\mathcal{T}_h^{\Omega_1}). \tag{58}$$

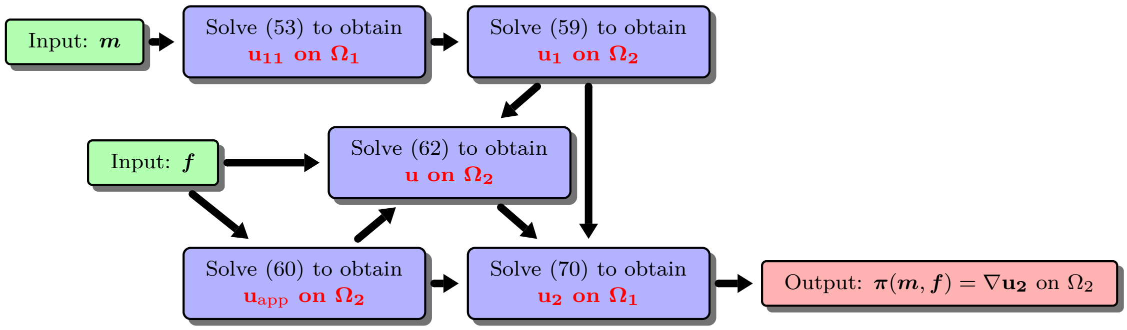

FIGURE 3. Overview on the computation of $\boldsymbol{\pi}(\boldsymbol{m},\boldsymbol{f}) = \nabla u_2$ on Ω_1.

The next statement proves that indeed the strayfield contribution is covered by our approach.

Proposition 17. *The operator* $\boldsymbol{\pi}_h(\boldsymbol{m}) = S_h(\boldsymbol{m}) := \nabla u_{11h} + \nabla u_{12h}$ *defined via* (57)–(58) *satisfies* $\boldsymbol{\pi}_h \in L(\boldsymbol{L}^2(\Omega_1); \boldsymbol{L}^2(\Omega_1))$, *and convergence* (42) *towards* $\boldsymbol{\pi}(\boldsymbol{m}) = S(\boldsymbol{m}) := \nabla u_1$ *holds even strongly in* $\boldsymbol{L}^2(\Omega_1)$. *In particular, Lemma 15 applies and guarantees the assumptions* (31)–(32) *of Theorem 7.*

Proof. First, note that the FE solution u_{11h} of (57) is a Galerkin approximation of (53). Therefore, stability proves $\|\nabla u_{11h}\|_{\boldsymbol{L}^2(\Omega_1)} \le \|\nabla u_{11}\|_{\boldsymbol{L}^2(\Omega_1)} \le \|\boldsymbol{m}\|_{\boldsymbol{L}^2(\Omega_1)}$ as well as $\|\nabla(u_{11} - u_{11h})\|_{\boldsymbol{L}^2(\Omega_1)} \to 0$ as $h \to 0$ by density arguments.

Second, we exploit the Céa-type estimate for inhomogeneous Dirichlet problems which states

$$\|\nabla(u_{12} - u_{12h})\|_{\boldsymbol{L}^2(\Omega_1)} \le \min_{\substack{w_h \in \mathcal{S}^1(\mathcal{T}_h^{\Omega_1}) \\ w_h|_\Gamma = I_h^{\Gamma_1}(K_1 - 1/2)u_{11h}^{\mathrm{int}}}} \|\nabla(u_{12} - w_h)\|_{\boldsymbol{L}^2(\Omega_1)}.$$

We now plug in $u_{12} = \widetilde{K}_1(u_{11}^{\mathrm{int}})$ and $w_h = I_h^{\Omega_1}\widetilde{K}_1(u_{11h}^{\mathrm{int}})$ to see

$$\begin{aligned}\|\nabla(u_{12} - u_{12h})\|_{\boldsymbol{L}^2(\Omega_1)} &\le \|\widetilde{K}_1(u_{11}^{\mathrm{int}}) - I_h^{\Omega_1}\widetilde{K}_1(u_{11h}^{\mathrm{int}})\|_{H^1(\Omega_1)} \\ &\le \|(1 - I_h^{\Omega_1})\widetilde{K}_1(u_{11}^{\mathrm{int}})\|_{H^1(\Omega_1)} + \|I_h^{\Omega_1}\widetilde{K}_1(u_{11}^{\mathrm{int}} - u_{11h}^{\mathrm{int}})\|_{H^1(\Omega_1)}.\end{aligned}$$

From the projection property and stability of $I_h^{\Omega_1}$ we get

$$\|(1 - I_h^{\Omega_1})\widetilde{K}_1(u_{11}^{\mathrm{int}})\|_{H^1(\Omega_1)} \lesssim \min_{w_h \in \mathcal{S}^1(\mathcal{T}_h^{\Omega_1})} \|\widetilde{K}_1(u_{11}^{\mathrm{int}}) - w_h\|_{H^1(\Omega_1)} \xrightarrow{h\to 0} 0.$$

For the other term, we use continuity of $I_h^{\Omega_1}$ and $\widetilde{K}_1$ as well as Poincaré's estimate to conclude

$$\|I_h^{\Omega_1}\widetilde{K}_1(u_{11}^{\mathrm{int}} - u_{11h}^{\mathrm{int}})\|_{H^1(\Omega_1)} \lesssim \|u_{11} - u_{11h}\|_{H^1(\Omega_1)} \lesssim \|\nabla(u_{11} - u_{11h})\|_{\boldsymbol{L}^2(\Omega_1)} \xrightarrow{h\to 0} 0$$

with the above estimate. Since this analysis was particularly independent of $\boldsymbol{m}$, the triangle inequality finally yields

$$\|S_h\boldsymbol{m} - S\boldsymbol{m}\|_{\boldsymbol{L}^2(\Omega_1)} \le \|\nabla(u_{11} - u_{11h})\|_{\boldsymbol{L}^2(\Omega_1)} + \|\nabla(u_{12} - u_{12h})\|_{\boldsymbol{L}^2(\Omega_1)} \to 0$$

for all $\boldsymbol{m} \in X = \boldsymbol{L}^2(\Omega_1)$. The first part of Lemma 15 thus yields the boundedness $\|\boldsymbol{\pi}_h(\boldsymbol{n})\|_{\boldsymbol{L}^2(\Omega_1)}$ for all $\boldsymbol{n} \in \boldsymbol{L}^2(\Omega_1)$ with $|\boldsymbol{n}| \le 1$ almost everywhere. Hence, from part (a) of Theorem 7 we get strong $\boldsymbol{L}^2(\Omega_\tau)$ subconvergence of the operands. Application of Lemma 15 finally concludes the proof. ∎

4.6. **Application: Multiscale approach for total magnetic field.** Our aim is to apply Proposition 15 to the model problem posed in Section 1, i.e. the computation of $\boldsymbol{\pi}(\boldsymbol{m}, \boldsymbol{f}) = \nabla u_2$ on Ω_1. In the following we consider the subproblems needed for the computation of ∇u_2 as well as their discretizations. An overview illustration is given in Figure 3.

4.6.1. *Continuous formulation.* The computation of the total potential u, and therefore of u_2, relies on the computation of the auxiliary potential u_{app} and the strayfield potential on Ω_2. For a magnetization $\boldsymbol{m} \in \boldsymbol{L}^2(\Omega_1)$, we compute $u_1 \in H^1(\Omega_1)$ via Section 4.5.1 as solution of the strayfield operator on the microscopic part. Recall $u_1 = u_{12} = \widetilde{K}_1 u_{11}^{\text{int}}$ is defined in Section 4.5.1 on $\mathbb{R}^3 \backslash \overline{\Omega}_1$ with $u_{11} \in H^1_*(\Omega_1)$ being the solution of (53). According to (48), u_1 on Ω_2 solves the inhomogeneous Dirichlet problem

$$\begin{aligned} -\Delta u_1 &= 0 && \text{in } \Omega_2, \\ u_1^{\text{int}} &= \Big(\widetilde{K}_1 u_{11}^{\text{int}}\Big)^{\text{int}} && \text{on } \Gamma_2. \end{aligned} \tag{59}$$

For the auxiliary potential u_{app}, the non-dimensional version of (11) reads

$$\begin{aligned} \Delta u_{\text{app}} &= 0 && \text{in } \Omega_2, \\ \partial_{\boldsymbol{\nu}} u_{\text{app}}^{\text{int}} &= -\boldsymbol{f} \cdot \boldsymbol{\nu} && \text{on } \Gamma_2, \end{aligned} \tag{60}$$

with $\nabla u_{\text{app}} = -\boldsymbol{f}$ in Ω_2. With respect to the abstract notation of Lemma 15, we introduce the continuous linear operator

$$\begin{aligned} &\widetilde{T} : \boldsymbol{L}^2(\Omega_1) \times \boldsymbol{H}(\text{div}; \Omega_2) \to H^{1/2}(\Gamma_2) \times H^{-1/2}(\Gamma_2), \\ &\widetilde{T}(\boldsymbol{m}, \boldsymbol{f}) = (u_1^{\text{int}} + u_{\text{app}}^{\text{int}}, \boldsymbol{f} \cdot \boldsymbol{\nu} - \partial_{\boldsymbol{\nu}} u_1^{\text{int}}). \end{aligned} \tag{61}$$

The space Y from Lemma 15 is thus given by $\boldsymbol{H}(\text{div}; \Omega_2)$.

In the next step, we then compute the total magnetostatic potential $u = u_1 + u_2 + u_{\text{app}}$ related to the macroscopic domain Ω_2. With $\widetilde{\chi}(|\nabla u|) = \chi\Big(M_s|\boldsymbol{f} - \nabla u_1 - \nabla u_2|\Big)$, the non-dimensional form of (12) is equivalently stated by means of the Johnson-Nédélec coupling from [19],

$$\begin{aligned} \int_{\Omega_2} (1 + \widetilde{\chi}(|\nabla u|)) \nabla u \cdot \nabla v - \int_{\Gamma_2} \phi v &= -\int_{\Gamma_2} (\boldsymbol{f} \cdot \boldsymbol{\nu} - \partial_{\boldsymbol{\nu}} u_1^{\text{ext}})\, v, \\ V_2 \phi - (K_2 - 1/2) u^{\text{int}} &= -(K_2 - 1/2)(u_1^{\text{int}} + u_{\text{app}}^{\text{int}}), \end{aligned} \tag{62}$$

for all $v \in H^1(\Omega_2)$, see [4] for the nonlinear case and [19, 25] for the linear one. In the second equation, $V_2 : H^{-1/2}(\Gamma_2) \to H^{1/2}(\Gamma_2)$ and $K_2 : H^{1/2}(\Gamma_2) \to H^{1/2}(\Gamma_2)$ denote the simple-layer potential and the double-layer potential with respect to Γ_2. The coupling formulation provides the total potential u on Ω_2 as well as the exterior normal derivative $\phi = \partial_{\boldsymbol{\nu}} u_2^{\text{ext}}$ of u_2 on Γ_2.

Recall that the dual space $H^{-1/2}(\Gamma_2)$ of the trace space $H^{1/2}(\Gamma_2)$ is continuously embedded into the dual space $\widetilde{H}^{-1}(\Omega_2)$ of $H^1(\Omega_2)$ by means of the trace operator which maps $H^1(\Omega_2)$ onto $H^{1/2}(\Gamma_2)$. Therefore, the operator $\widetilde{T}$ from (61) can also be considered as an operator to $H^{1/2}(\Gamma_2) \times \widetilde{H}^{-1}(\Omega_2)$. With respect to the abstract notation of Lemma 15, the coupling formulation (62) gives rise to the nonlinear operator

$$\begin{aligned} &\widetilde{A} : H^{-1/2}(\Gamma_2) \times H^1(\Omega_2) \to H^{1/2}(\Gamma_2) \times \widetilde{H}^{-1}(\Omega_2) \\ &\widetilde{A}(\phi, u) = (u_1^{\text{int}} + u_{\text{app}}^{\text{int}}, \boldsymbol{f} \cdot \boldsymbol{\nu} - \partial_{\boldsymbol{\nu}} u_1^{\text{ext}}). \end{aligned} \tag{63}$$

Solvability of the Johnson-Nédélec coupling equations (62)–(63) hinges strongly on the material law χ. The following lemma characterizes sufficient conditions such that the nonlinear part of (62) is strongly monotone and Lipschitz continuous.

Lemma 18. *Let $\widetilde{\chi} : \mathbb{R}_{\geq 0} \to \mathbb{R}$ be a continuous function such that the function*

$$g : \mathbb{R}_{\geq 0} \to \mathbb{R}, \quad g(t) = t + \widetilde{\chi}(t)t$$

is differentiable and fulfills

$$g'(t) \in [\gamma, L] \quad \text{for all } t \geq 0 \tag{64}$$

with constants $L \geq \gamma > 0$. Then, the (nonlinear) operator

$$\mathcal{A} : \boldsymbol{L}^2(\Omega_2) \to \boldsymbol{L}^2(\Omega_2), \quad \mathcal{A}\mathbf{w} = (1 + \widetilde{\chi}(|\mathbf{w}|))\mathbf{w} \tag{65}$$

is Lipschitz continuous and strongly monotone, i.e. there holds

$$\|\mathcal{A}\mathbf{u} - \mathcal{A}\mathbf{v}\|_{\boldsymbol{L}^2(\Omega_2)} \leq L\|\mathbf{u} - \mathbf{v}\|_{\boldsymbol{L}^2(\Omega_2)}$$
$$\langle \mathcal{A}\mathbf{u} - \mathcal{A}\mathbf{v}\,;\, \mathbf{u} - \mathbf{v}\rangle_{\Omega_2} \geq \gamma\|\mathbf{u} - \mathbf{v}\|^2_{\boldsymbol{L}^2(\Omega_2)}$$

for all $\mathbf{u}, \mathbf{v} \in \boldsymbol{L}^2(\Omega_2)$. □

We stress that the operator $\widetilde{A}$ is not uniformly monotone as e.g. the left-hand side of (62) is zero for $u = 1, \phi = 0$. Therefore, the Browder-Minty theorem is not applicable directly. In the following, we introduce an equivalent formulation of equation (62)–(63), which turns out to fit into the setting of uniformly monotone operators. To that end, we need the linear operator $L : X^* \to X^*$ defined via

$$Lx^* = x^* + \langle x^*, (\mathbf{1}, 0)\rangle_{X^* \times X} \langle \widetilde{A}(\cdot, \cdot), (\mathbf{1}, 0)\rangle_{X^* \times X} \quad \text{for all } x^* \in X^*, \tag{66}$$

where $\mathbf{1} \in \mathcal{P}^0(\mathcal{E}_h^{\Gamma_2})$ denotes the constant function. As observed in [4, Section 4], the Johnson-Nédélec coupling equations can then be equivalently rewritten as follows:

Lemma 19. *The operator $L : X^* \to X^*$ from* (66) *is well-defined, linear, and continuous. Moreover, the pair $(\phi, u) \in X$ solves the operator formulation*

$$\widetilde{A}(\phi, u) = \widetilde{T}(\boldsymbol{m}, \boldsymbol{f}) \tag{67}$$

of (62) *if and only if*

$$A(\phi, u) = T(\boldsymbol{m}, \boldsymbol{f}), \tag{68}$$

where $A = L\widetilde{A}$ and $T = L\widetilde{T}$. In particular, $\widetilde{A}^{-1}\widetilde{T} = A^{-1}T$, and the operator T is linear, well-defined, and continuous. Under the assumptions of Lemma 18 with $\gamma > 1/4$, the operator $A = L\widetilde{A}$ is Lipschitz continuous and strongly monotone. In particular, it fulfills the assumptions of the Browder-Minty theorem for uniformly monotone operators. □

So far, we have computed the total potential u and by simple postprocessing $u_2 = u - u_1 - u_{\text{app}}$ on Ω_2. The effective field $\boldsymbol{h}_{\text{eff}}$, however, relies on the gradient of u_2 on the microscopic part Ω_1. Since u_2 solves $-\Delta u_2 = 0$ in $\mathbb{R}^3 \backslash \overline{\Omega}_2$, u_2 can be computed by means of the representation formula, cf. e.g. [24, Theorem 3.1.6],

$$u_2 = -\widetilde{V}_2(\partial_{\boldsymbol{\nu}} u_2^{\text{ext}}) + \widetilde{K}_2(u_2^{\text{ext}}) \quad \text{in } \mathbb{R}^3 \backslash \overline{\Omega}_2 \supset \Omega_1. \tag{69}$$

To lower the computational cost for an implementation, we will, however, not use the representation formula on Ω_1, but only on Γ_1 and solve an inhomogeneous Dirichlet problem instead. With $u_2^{\rm ext} = u_2^{\rm int} = u^{\rm int} - u_1^{\rm int} - u_{\rm app}^{\rm int}$ as well as $\phi = \partial_{\boldsymbol{\nu}} u_2^{\rm ext}$ on Γ_2, we obtain

$$
\begin{aligned}
-\Delta u_2 &= 0 && \text{in } \Omega_1,\\
u_2^{\rm int} &= \Big(-\widetilde{V}_2\phi + \widetilde{K}_2(u^{\rm int} - u_1^{\rm int} - u_{\rm app}^{\rm int})\Big)^{\rm int} && \text{on } \Gamma_1,
\end{aligned}
\tag{70}
$$

according to (48). Put into the abstract frame, we consider the linear and continuous operator

$$
\begin{aligned}
&S : H^{-1/2}(\Gamma_2) \times H^1(\Omega_2) \to \boldsymbol{L}^2(\Omega_1)\\
&S(\phi, u^{\rm int}) = \nabla u_2.
\end{aligned}
\tag{71}
$$

Overall, the computation of $\boldsymbol{\pi}(\boldsymbol{m}, \boldsymbol{f}) = S\widetilde{A}^{-1}\widetilde{T}(\boldsymbol{m}, \boldsymbol{f}) = SA^{-1}T = \nabla u_2$ on Ω_1 is therefore done in five steps: First, we compute u_{11} on Ω_1 as solution of (53). Second, (59) is solved to compute ∇u_1 on Ω_2. Third, (60) is solved to compute $u_{\rm app}$ on Ω_2. Fourth, (62) is solved to provide u and $\phi = \partial_{\boldsymbol{\nu}} u_2^{\rm ext}$ on Γ_2. Finally, (70) is solved to provide ∇u_2 on Ω_1.

Remark 20. *Note that the formal definition of the operator S once again requires the solution of* (59)–(60) *to provide $u_1^{\rm int} + u_{\rm app}^{\rm int}$. Theoretically, this can be dealt with by considering the extended operators*

$$
\begin{aligned}
\widehat{T}(\boldsymbol{m}, \boldsymbol{f}) &= (u_1^{\rm int} + u_{\rm app}^{\rm int}, \boldsymbol{f}\cdot\boldsymbol{\nu} - \partial_{\boldsymbol{\nu}} u_1^{\rm ext}, u_1^{\rm int} + u_{\rm app}^{\rm int}),\\
\widehat{A}(\phi, u, u_1^{\rm int} + u_{\rm app}^{\rm int}) &= (u_1^{\rm int} + u_{\rm app}^{\rm int}, \boldsymbol{f}\cdot\boldsymbol{\nu} - \partial_{\boldsymbol{\nu}} u_1^{\rm ext}, u_1^{\rm int} + u_{\rm app}^{\rm int}),\\
\widehat{S}(\phi, u, u_1^{\rm int} + u_{\rm app}^{\rm int}) &= \nabla u_2.
\end{aligned}
$$

Then, $\widehat{S}$ and $\widehat{T}$ are still linear and continuous. Provided A is uniformly monotone, the inverse of A is well-defined and continuous so that (an obvious extension of) Lemma 15 still applies.

Remark 21. *Finally, we give some examples of material laws $\widetilde{\chi}$, covered by Lemma 19:*
(i) Consider the material law

$$\widetilde{\chi}(t) = C_5 \tanh(C_6 t)/t \quad \textit{for } t > 0, \quad \widetilde{\chi}(0) = C_5 C_6$$

with dimensionless constants $C_5, C_6 > 0$. Then, $g(t) = t + C_5 \tanh C_6 t$ fulfills (64) *with $\gamma = 1$ and $L = 1 + C_5 C_6$.*
(ii) According to [23], *it is reasonable to approximate the magnetic susceptibility in terms of a rational function, i.e.*

$$\widetilde{\chi}(t) = \frac{C_7 + C_8 t}{1 + C_9 t + C_{10} t^2}$$

with certain, material-dependent constants $C_7, C_8, C_9, C_{10} > 0$. For typical materials, it holds (64) *with $\gamma = 1$ and some $L > 1$ that depends on C_7, C_8, C_9, C_{10}, cf.* [23, Table 1].

4.6.2. *Discretization of $\widetilde{T}$.* As for the strayfield, we solve (57) to obtain an approximation $u_{11h} \in \mathcal{S}^1_*(\mathcal{T}_h^{\Omega_1})$ of u_{11}. Next, we proceed as in Section 4.5 and discretize the given Dirichlet data by means of the Scott-Zhang operator. Note that $u_1 = \widetilde{K}_1 u_{11}^{\rm int} \in C^\infty(\mathbb{R}^3 \backslash \overline{\Omega}_1) \subset H^2(\Omega_2)$. Therefore, the discretization of (59) then reads: Find $u_{1h} \in \mathcal{S}^1(\mathcal{T}_h^{\Omega_2})$ such that

$$\int_{\Omega_2} \nabla u_{1h} \cdot \nabla v_h \, dx = 0 \quad \text{for all } v_h \in \mathcal{S}^1_0(\mathcal{T}_h^{\Omega_2}) \quad \text{with } u_{1h}|_{\Gamma_2} = I_h^{\Gamma_2} K_1 u_{11h}^{\rm int}. \tag{72}$$

Arguing as in the proof of Proposition 17, one obtains the following result:

Lemma 22. *The operator $B_h : \boldsymbol{L}^2(\Omega_1) \to \mathcal{S}^1(\mathcal{T}_h^{\Omega_2})$ with $B_h \boldsymbol{m} := u_{1h}$, which uses the discrete solution of* (57) *to compute the solution $u_{1h} \in \mathcal{S}^1(\mathcal{T}_h^{\Omega_2})$ of* (72)*, is well-defined, linear, and continuous. Moreover, there holds strong convergence $B_h \boldsymbol{m} \to B\boldsymbol{m}$ in $H^1(\Omega_2)$ as $h \to 0$ for all $\boldsymbol{m} \in \boldsymbol{L}^2(\Omega_1)$. Here, $B : \boldsymbol{L}^2(\Omega_1) \to H^1(\Omega_2)$ denotes the linear and continuous solution operator of* (59)*.* □

The discrete version of (60) reads as follows: Let $u_{\mathrm{app},h} \in \mathcal{S}^1_*(\mathcal{T}_h^{\Omega_2})$ solve

$$\int_{\Omega_2} \nabla u_{\mathrm{app},h} \cdot \nabla v_h \, dx = -\int_{\Gamma_2} \boldsymbol{f} \cdot \boldsymbol{\nu} \, d\Gamma_2 \quad \text{for all } v_h \in \mathcal{S}^1_*(\mathcal{T}_h^{\Omega_2}). \tag{73}$$

The following result is well-known.

Lemma 23. *Let Ω_1 be convex. Then, the operator $B_h : \boldsymbol{H}(\mathrm{div};\Omega_2) \to \mathcal{S}^1_*(\mathcal{T}_h^{\Omega_2})$ which maps $\boldsymbol{f}$ to the discrete solution of* (73) *is well-defined, linear, and continuous. Moreover, there holds strong convergence $B_h\boldsymbol{f} \to B\boldsymbol{f}$ in $H^1(\Omega_2)$ as $h \to 0$ for all $\boldsymbol{f} \in \boldsymbol{H}(\mathrm{div},\Omega_2)$. Here, $B : \boldsymbol{H}(\mathrm{div};\Omega_2) \to H^1_*(\Omega_2)$ denotes the linear and continuous solution operator of* (60)*.* □

Recall that $u_1 \in C^\infty(\mathbb{R}^3 \backslash \overline{\Omega}_1) \subseteq H^2(\Omega_2)$, cf. (48). Therefore, we can replace $\partial_{\boldsymbol{\nu}} u_1^{\mathrm{ext}}$ by $\partial_{\boldsymbol{\nu}} u_1^{\mathrm{int}}$ on the right-hand side of (62). With respect to the definition of the operator $\widetilde{T}$ in (61), it remains to prove convergence $\partial_{\boldsymbol{\nu}} u_{1h}^{\mathrm{int}} \to \partial_{\boldsymbol{\nu}} u_1^{\mathrm{int}}$ strongly in $H^{-1/2}(\Gamma_2)$ as $h \to 0$. To that end, let $u_{1h}^\star$ be the discrete solution of (72) with boundary data $u_{1h}^\star|_{\Gamma_2} = I_h^{\Gamma_2} K_1 u_{11}^{\mathrm{int}}$. As in Section 4.5.2, $I_h^{\Gamma_2} : H^{1/2}(\Gamma_2) \to \mathcal{S}^1(\mathcal{T}_h^{\Omega_2}|_{\Gamma_2})$ denotes the projection induced by the Scott-Zhang projection $I_h^{\Omega_2} : H^1(\Omega_2) \to \mathcal{S}^1(\mathcal{T}_h^{\Omega_2})$, now considered on Ω_2 instead of Ω_1. As is the proof of Proposition 17, the Céa lemma proves

$$\|u_1 - u_{1h}^\star\|_{H^1(\Omega_2)} \lesssim \|u_1 - I_h^{\Omega_2} u_1\|_{H^1(\Omega_2)} = \mathcal{O}(h).$$

For the term $\|u_{1h} - u_{1h}^\star\|_{H^1(\Omega_2)}$, we get due to convexity of Ω_1 and thus $u_1 \in H^2(\Omega_1)$

$$\|u_{1h}^\star - u_{1h}\|_{H^1(\Omega_2)} \lesssim \|u_{11}^{\mathrm{int}} - u_{11h}^{\mathrm{int}}\|_{H^{1/2}(\Gamma_1)} \lesssim \|u_{11} - u_{11h}\|_{H^1(\Omega_1)} = \mathcal{O}(h),$$

where we have used stability of $I_h^{\Omega_2}$ and $\widetilde{K}_1$. Altogether, we see

$$\|u_1 - u_{1h}\|_{H^1(\Omega_2)} \le \|u_1 - u_{1h}^\star\|_{H^1(\Omega_2)} + \|u_{1h}^\star - u_{1h}\|_{H^1(\Omega_2)} = \mathcal{O}(h).$$

The desired result now follows from the next lemma and $\|\Psi\|_{H^{-1/2}(\Gamma_2)} \le \|\Psi\|_{L^2(\Gamma_2)}$ for all $\Psi \in L^2(\Gamma_2)$.

Lemma 24. *Let $w \in H^2(\Omega_2)$ with $\partial_\nu w \in L^2(\Gamma_2)$ and let $w_h \in \mathcal{S}^1(\mathcal{T}_h^{\Omega_2})$ be a sequence with*

$$\|\nabla(w - w_h)\|_{L^2(\Omega_2)} \le C_{11} h^{1/2+\varepsilon} \quad \textit{for all } h > 0$$

for some h-independent constants $C_{11} > 0$ and $\varepsilon > 0$. Then, there holds

$$\|\partial_\nu(w - w_h)\|_{L^2(\Gamma_2)} \le C_{12} h^\varepsilon \quad \textit{for all } h > 0$$

and a constant $C_{12} > 0$ which is independent of $h > 0$.

Proof. According to the trace-inequality (e.g. [12, Lemma 3.4]), it holds for any face $E \subset \Gamma_2$ with corresponding element $T \in \mathcal{T}_h^{\Omega_2}$ (i.e. $E \subset \partial T$)

$$\|\partial_\nu(w - w_h)\|^2_{\boldsymbol{L}^2(\partial T \cap \Gamma_2)} \lesssim h^{-1} \|\nabla(w - w_h)\|^2_{\boldsymbol{L}^2(T)} + \|\nabla(w - w_h)\|_{\boldsymbol{L}^2(T)} \|D^2(w - w_h)\|_{\boldsymbol{L}^2(T)}$$

With $D^2 w_h = 0$ on T and by summing over all faces E in the boundary Γ_2, we end up with

$$\begin{aligned}\|\partial_\nu(w-w_h)\|^2_{\boldsymbol{L}^2(\Gamma_2)} &\lesssim h^{-1}\|\nabla(w-w_h)\|^2_{\boldsymbol{L}^2(\Omega_2)} + \|\nabla(w-w_h)\|_{\boldsymbol{L}^2(\Omega_2)}\|D^2 w\|_{\boldsymbol{L}^2(\Omega_2)}\\ &= \mathcal{O}(h^\varepsilon).\end{aligned}$$

This concludes the proof. □

Combining Lemma 22–24, we obtain the following proposition.

Proposition 25. *With $X = H^{-1/2}(\Gamma_2)\times H^1(\Omega_2)$ and $Y = \boldsymbol{H}(\mathrm{div}\,;\Omega_2)$, the operator*

$$\begin{aligned}&\widetilde{T}_h : \boldsymbol{L}^2(\Omega_1)\times \boldsymbol{H}(\mathrm{div}\,;\Omega_2) \to \mathcal{P}^0(\mathcal{E}_h^{\Gamma_2})\times \mathcal{S}^1(\mathcal{T}_h^{\Omega_2}) \subseteq X^*,\\ &\widetilde{T}_h(\boldsymbol{m},\boldsymbol{f}) = (u_{1h}^{\mathrm{int}} + u_{\mathrm{app},h}^{\mathrm{int}}, \boldsymbol{f}\cdot\boldsymbol{\nu} - \partial_{\boldsymbol{\nu}} u_{1h}^{\mathrm{int}})\end{aligned} \tag{74}$$

is well-defined, linear, and continuous and satisfies (43) *with (T_h, T) replaced by $(\widetilde{T}_h, \widetilde{T})$.* □

4.6.3. *Discretization of $\widetilde{A}$ and equivalent formulation.* For the numerical solution of (62), we use lowest-order finite elements combined with lowest-order boundary elements. The numerical approximation of the Johnson-Nédélec equations reads as follows: Find $(\phi_h, u_h) \in X_h := \mathcal{P}^0(\mathcal{E}_h^{\Gamma_2})\times\mathcal{S}^1(\mathcal{T}_h^{\Omega_2})$ such that

$$\begin{aligned}\int_{\Omega_2}(1+\widetilde{\chi}(|\nabla u_h|))\nabla u_h\cdot\nabla v_h - \int_{\Gamma_2}\phi_h v_h^{\mathrm{int}} &= -\int_{\Omega_2}(\boldsymbol{f}\cdot\boldsymbol{\nu} - \partial_{\boldsymbol{\nu}} u_{1h}^{\mathrm{int}})v_h,\\ \int_{\Gamma_2}(V_2\phi_h - (K_2 - 1/2)u_h^{\mathrm{int}})\psi_h &= -\int_{\Gamma_2}(K_2-1/2)(u_{1h}^{\mathrm{int}} + u_{\mathrm{app},h}^{\mathrm{int}})\psi_h\end{aligned} \tag{75}$$

for all $(\psi_h, v_h) \in X_h$, where $(u_{\mathrm{app},h}, u_{1h})$ is the output of T_h. With the operator $\widetilde{A}$ from (63), the Galerkin formulation (75) can be rewritten as

$$\langle \widetilde{A}(\phi_h,u_h),(\psi_h,v_h)\rangle_{X_h^*\times X_h} = \langle \widetilde{T}_h(\boldsymbol{m},\boldsymbol{f}),(\psi_h,v_h)\rangle_{X_h^*\times X_h} \quad \text{for all } (\psi_h,v_h)\in X_h. \tag{76}$$

It is proved in [4, Section 4] that Lemma 19 does not only cover the continuous setting, but also applies for the Galerkin formulation. In particular (76) is equivalent to

$$\langle A(\phi_h,u_h),(\psi_h,v_h)\rangle_{X_h^*\times X_h} = \langle T_h(\boldsymbol{m},\boldsymbol{f}),(\psi_h,v_h)\rangle_{X_h^*\times X_h} \quad \text{for all } (\psi_h,v_h)\in X_h, \tag{77}$$

with $A = L\widetilde{A}, T_h = L\widetilde{T}_h$ and L from (66). Consequently, T_h satisfies assumption (43).

Remark 26. *The equivalent formulations introduced in Proposition 19 are only used for theoretical considerations. In practice,* (75) *is solved directly.*

4.6.4. *Discretization of S.* In analogy to (72), we use the Scott-Zhang operator $I_h^{\Gamma_1}$ to discretize the Dirichlet data in (70). The corresponding discretization thus reads: *Find $u_{2h}\in\mathcal{S}^1(\mathcal{T}_h^{\Omega_1})$ with $u_{2h}|_{\Gamma_1} = I_h^{\Gamma_1}\Big(-\widetilde{V}_2\phi_h + \widetilde{K}_2(u_h^{\mathrm{int}} - u_{1h}^{\mathrm{int}} - u_{\mathrm{app},h}^{\mathrm{int}})\Big)^{\mathrm{int}}$ such that*

$$\int_{\Omega_1}\nabla u_{2h}\cdot\nabla v_h = 0 \quad \text{for all } v_h\in\mathcal{S}_0^1(\mathcal{T}_h^{\Omega_1}). \tag{78}$$

In complete analogy to the previous results, we get the following:

Lemma 27. *The operator $S_h : X = H^{-1/2}(\Gamma_2)\times H^1(\Omega_2)\to\mathcal{P}^0(\mathcal{T}_h^{\Omega_1})^3 \subseteq \boldsymbol{L}^2(\Omega_1)$, which computes the gradient of the solution of* (78) *is well-defined, linear, and continuous. Moreover, there holds strong convergence $S_h x \to Sx$ strongly in $\boldsymbol{L}^2(\Omega_1)$ as $h\to 0$ for all $x\in X$. Here, $S : X\to\boldsymbol{L}^2(\Omega_1)$ denotes the exact solution operator of* (70). □

Altogether, we get the following result:

Proposition 28. *Assume that the microscopic domain Ω_1 is convex, that the macroscopic domain Ω_2 is simply connected, and that the material law χ fulfills the conditions of Lemma 18. Let $Y := \boldsymbol{H}(\mathrm{div}\,;\Omega_2)$ and $\zeta_{hk}^- := \boldsymbol{f}_{hk}^-$. Assume further that $\boldsymbol{f}|_{\Omega_2}$ is sufficiently smooth, such that $\boldsymbol{f}_{hk}^- \to \boldsymbol{f}$ strongly in $L^2\Big(\boldsymbol{H}(\mathrm{div}\,;\Omega_2)\Big)$ and $\boldsymbol{f}_{hk}^- \in L^\infty\Big(\boldsymbol{H}(\mathrm{div}\,;\Omega_2)\Big)$. Then, the operator $\boldsymbol{\pi}_h(\boldsymbol{m},\boldsymbol{f}) = S_h A^{-1} T_h(\boldsymbol{m},\boldsymbol{f}) = \nabla u_{2h}$ defined via the previous section satisfies all assumptions of Lemma 15. In particular, the assumptions* (31)–(32) *of Theorem 7 are satisfied.* □

Appendix A. Energy estimate

The following energy estimate can be obtained under certain assumptions on the general energy contributions $\boldsymbol{\pi}_h(\cdot)$. Independently of the concrete multiscale setting, this might be of general interest. Note that in this section, we neglect a possible dependence of $\boldsymbol{\pi}(\cdot)$ on a second quantity ζ.

Lemma 29 (improved energy estimate)**.** *Let $\boldsymbol{\pi}_h(\cdot)$ be uniformly Lipschitz continuous and let the applied field $\boldsymbol{f} \in \boldsymbol{L}^4(\Omega_\tau)$ be constant in time, i.e. $\boldsymbol{f}_h^j = \boldsymbol{f}$ for all time steps in Algorithm 5. Furthermore, let $\boldsymbol{\pi}_h(\cdot)$ satisfy $\|\boldsymbol{\pi}_h(\boldsymbol{n})\|_{\boldsymbol{L}^4(\Omega_1)} \le C_{13}$, with $C_{13} > 0$ independent of $h > 0$ and $\boldsymbol{n} \in \boldsymbol{L}^2(\Omega_1)$ with $|\boldsymbol{n}| \le 1$ almost everywhere. Then, the energy*

$$\mathcal{E}\Big(\boldsymbol{m}(t)\Big) := C_{\mathrm{exch}}\|\nabla\boldsymbol{m}(t)\|^2_{\boldsymbol{L}^2(\Omega_1)} + \langle\boldsymbol{\pi}(\boldsymbol{m}(t)),\boldsymbol{m}(t)\rangle - \langle\boldsymbol{f}(t),\boldsymbol{m}(t)\rangle \tag{79}$$

satisfies

$$\mathcal{E}\Big(\boldsymbol{m}(t)\Big) + 2(\alpha-\varepsilon)\|\boldsymbol{m}_\tau\|^2_{\boldsymbol{L}^2(\Omega_t)} \le \mathcal{E}\Big(\boldsymbol{m}(0)\Big) + \frac{C_{14}}{\varepsilon}\|\boldsymbol{f}\|_{\boldsymbol{L}^2(\Omega_\tau)} + \frac{C_{15}}{\varepsilon} \tag{80}$$

for any $\varepsilon > 0$ and almost every $t \in [0,\tau_{\mathrm{end}}]$. Here, the constants $C_{14}, C_{15} > 0$ depend only on the Lipschitz constant of $\boldsymbol{\pi}_h$ and $|\Omega_1|$. In addition, for vanishing applied field $\boldsymbol{f}$ and self-adjoint operators $\boldsymbol{\pi}_h(\cdot)$, it even holds that

$$\mathcal{E}\Big(\boldsymbol{m}(t)\Big) + 2\alpha\|\boldsymbol{m}_\tau\|^2_{\boldsymbol{L}^2(\Omega_t)} \le \mathcal{E}\Big(\boldsymbol{m}(0)\Big) \tag{81}$$

for almost every $t \in [0,\tau_{\mathrm{end}}]$.

Proof. To abbreviate notation, we define

$$H_h(\boldsymbol{m}_h^i) := \boldsymbol{\pi}_h(\boldsymbol{m}_h^i) - \boldsymbol{f}_h^i = \boldsymbol{\pi}_h(\boldsymbol{m}_h^i) - \boldsymbol{f}.$$

From the stability estimate (34), we get

$$\begin{aligned}
&\mathcal{E}(\boldsymbol{m}_h^{i+1}) - \mathcal{E}(\boldsymbol{m}_h^i)\\
&\qquad = C_{\mathrm{exch}}\|\nabla\boldsymbol{m}_h^{i+1}\|^2_{\boldsymbol{L}^2(\Omega_1)} + \langle H_h(\boldsymbol{m}_h^{i+1}),\boldsymbol{m}_h^{i+1}\rangle - C_{\mathrm{exch}}\|\nabla\boldsymbol{m}_h^i\|^2_{\boldsymbol{L}^2(\Omega_1)} - \langle H_h(\boldsymbol{m}_h^i),\boldsymbol{m}_h^i\rangle\\
&\qquad \le C_{\mathrm{exch}}\|\nabla\boldsymbol{m}_h^i\|^2_{\boldsymbol{L}^2(\Omega_1)} - 2C_{\mathrm{exch}}(\theta-1/2)k^2\|\nabla\boldsymbol{v}_h^i\|^2_{\boldsymbol{L}^2(\Omega_1)} - 2\alpha k\|\boldsymbol{v}_h^i\|^2_{\boldsymbol{L}^2(\Omega_1)}\\
&\qquad\quad - 2k\langle H_h(\boldsymbol{m}_h^i),\boldsymbol{v}_h^i\rangle + \langle H_h(\boldsymbol{m}_h^{i+1}),\boldsymbol{m}_h^{i+1}\rangle - C_{\mathrm{exch}}\|\nabla\boldsymbol{m}_h^i\|^2_{\boldsymbol{L}^2(\Omega_1)} - \langle H_h(\boldsymbol{m}_h^i),\boldsymbol{m}_h^i\rangle\\
&\qquad = -2C_{\mathrm{exch}}(\theta-1/2)k^2\|\nabla\boldsymbol{v}_h^i\|^2_{\boldsymbol{L}^2(\Omega_1)} - 2\alpha k\|\boldsymbol{v}_h^i\|^2_{\boldsymbol{L}^2(\Omega_1)} - 2k\langle H_h(\boldsymbol{m}_h^i),\boldsymbol{v}_h^i\rangle\\
&\qquad\quad + \langle H_h(\boldsymbol{m}_h^{i+1}) + H_h(\boldsymbol{m}_h^i),\boldsymbol{m}_h^{i+1}-\boldsymbol{m}_h^i\rangle + \langle H_h(\boldsymbol{m}_h^{i+1}),\boldsymbol{m}_h^i\rangle - \langle H_h(\boldsymbol{m}_h^i),\boldsymbol{m}_h^{i+1}\rangle.
\end{aligned}$$

Straightforward calculations now show

$$\begin{aligned}
&-2k\langle H_h(\boldsymbol{m}_h^i),\boldsymbol{v}_h^i\rangle + \langle H_h(\boldsymbol{m}_h^{i+1}) + H_h(\boldsymbol{m}_h^i),\boldsymbol{m}_h^{i+1}-\boldsymbol{m}_h^i\rangle\\
&\qquad\qquad = 2\langle H_h(\boldsymbol{m}_h^i),\boldsymbol{m}_h^{i+1}-\boldsymbol{m}_h^i-k\boldsymbol{v}_h^i\rangle + \langle H_h(\boldsymbol{m}_h^{i+1}) - H_h(\boldsymbol{m}_h^i),\boldsymbol{m}_h^{i+1}-\boldsymbol{m}_h^i\rangle.
\end{aligned}$$

Exploiting uniform boundedness of $H_h(\boldsymbol{m}_h^i)$ in $\boldsymbol{L}^4(\Omega_1)$ in combination with $|\boldsymbol{m}_h^{i+1} - \boldsymbol{m}_h^i - k\boldsymbol{v}_h^i| \le k^2|\boldsymbol{v}_h^i|^2/2$, cf. (37), we get

$$
\begin{aligned}
2\langle H_h(\boldsymbol{m}_h^i), \boldsymbol{m}_h^{i+1} - \boldsymbol{m}_h^i - k\boldsymbol{v}_h^i\rangle &\le k^2\|H_h(\boldsymbol{m}_h^i)\|_{\boldsymbol{L}^4(\Omega_1)}\|(\boldsymbol{v}_h^i)^2\|_{\boldsymbol{L}^{4/3}(\Omega_1)} \\
&\lesssim k^2\|\boldsymbol{v}_h^i\|^2_{\boldsymbol{L}^{8/3}(\Omega_1)} \le k^2\|\boldsymbol{v}_h^i\|^2_{\boldsymbol{L}^3(\Omega_1)}.
\end{aligned}
$$

Next, we make use of the Sobolev embedding (see [11])

$$
\|\boldsymbol{v}_h^i\|^2_{\boldsymbol{L}^3(\Omega_1)} \lesssim \|\boldsymbol{v}_h^i\|_{\boldsymbol{H}^1(\Omega_1)}\|\boldsymbol{v}_h^i\|_{\boldsymbol{L}^2(\Omega_1)}
$$

and see

$$
2\langle H_h(\boldsymbol{m}_h^i), \boldsymbol{m}_h^{i+1} - \boldsymbol{m}_h^i - k\boldsymbol{v}_h^i\rangle \lesssim k^2\|\boldsymbol{v}_h^i\|_{\boldsymbol{L}^2(\Omega_1)}\Big(\|\boldsymbol{v}_h^i\|_{\boldsymbol{L}^2(\Omega_1)} + \|\nabla\boldsymbol{v}_h^i\|_{\boldsymbol{L}^2(\Omega_1)}\Big).
$$

Using Lipschitz-continuity of $H_h(\cdot)$, i.e. of $\boldsymbol{\pi}_h(\cdot)$ and the fact that $\boldsymbol{f}_h^{j+1} = \boldsymbol{f}_h^j$, we further estimate

$$
\begin{aligned}
\langle H_h(\boldsymbol{m}_h^{i+1}) - H_h(\boldsymbol{m}_h^i), \boldsymbol{m}_h^{i+1} - \boldsymbol{m}_h^i\rangle &\le \|H_h(\boldsymbol{m}_h^{i+1}) - H_h(\boldsymbol{m}_h^i)\|_{\boldsymbol{L}^2(\Omega_1)}\|\boldsymbol{m}_h^{i+1} - \boldsymbol{m}_h^i\|_{\boldsymbol{L}^2(\Omega_1)} \\
&\lesssim \|\boldsymbol{m}_h^{i+1} - \boldsymbol{m}_h^i\|^2_{\boldsymbol{L}^2(\Omega_1)} \lesssim k^2\|\boldsymbol{v}_h^i\|^2_{\boldsymbol{L}^2(\Omega_1)}.
\end{aligned}
$$

Altogether, we thus have shown

$$
\begin{aligned}
\mathcal{E}(\boldsymbol{m}_h^{i+1}) - \mathcal{E}(\boldsymbol{m}_h^i) \le{} & -C_{\mathrm{exch}}2(\theta - 1/2)k^2\|\nabla\boldsymbol{v}_h^i\|^2_{\boldsymbol{L}^2(\Omega_1)} \\
& + Ck^2\Big(\|\boldsymbol{v}_h^i\|_{\boldsymbol{L}^2(\Omega_1)}\|\nabla\boldsymbol{v}_h^i\|_{\boldsymbol{L}^2(\Omega_1)} + \|\boldsymbol{v}_h^i\|^2_{\boldsymbol{L}^2(\Omega_1)}\Big) \\
& - 2\alpha k\|\boldsymbol{v}_h^i\|^2_{\boldsymbol{L}^2(\Omega_1)} + \langle H_h(\boldsymbol{m}_h^{i+1}), \boldsymbol{m}_h^i\rangle - \langle H_h(\boldsymbol{m}_h^i), \boldsymbol{m}_h^{i+1}\rangle,
\end{aligned} \tag{82}
$$

for some constant $C > 0$ which depends only on C_{13} and the Lipschitz constant of $\boldsymbol{\pi}_h$. Summation over $i = 0, \dots, j-1$ reveals for any $j = 0, \dots, N$ and for $\theta \in [1/2, 1]$

$$
\begin{aligned}
&\mathcal{E}(\boldsymbol{m}_h^j) - \mathcal{E}(\boldsymbol{m}_h^0) + 2\alpha k\sum_{i=0}^{j-1}\|\boldsymbol{v}_h^i\|^2_{\boldsymbol{L}^2(\Omega_1)} \\
&\qquad \le Ck\Big(\|\boldsymbol{v}_{hk}^-\|_{\boldsymbol{L}^2(\Omega_\tau)}\|\nabla\boldsymbol{v}_{hk}^-\|_{\boldsymbol{L}^2(\Omega_\tau)} + \|\boldsymbol{v}_{hk}^-\|^2_{\boldsymbol{L}^2(\Omega_\tau)}\Big) + \sum_{i=0}^{j-1}\langle H_h(\boldsymbol{m}_h^{i+1}), \boldsymbol{m}_h^i\rangle \\
&\qquad\quad - \sum_{i=0}^{j-1}\langle H_h(\boldsymbol{m}_h^i), \boldsymbol{m}_h^{i+1}\rangle \\
&\qquad = Ck\Big(\|\boldsymbol{v}_{hk}^-\|_{\boldsymbol{L}^2(\Omega_\tau)}\|\nabla\boldsymbol{v}_{hk}^-\|_{\boldsymbol{L}^2(\Omega_\tau)} + \|\boldsymbol{v}_{hk}^-\|^2_{\boldsymbol{L}^2(\Omega_\tau)}\Big) \\
&\qquad\quad + \sum_{i=0}^{j-1}\Big(\langle H_h(\boldsymbol{m}_h^{i+1}) - H_h(\boldsymbol{m}_h^i), \boldsymbol{m}_h^i\rangle - \langle H_h(\boldsymbol{m}_h^i), \boldsymbol{m}_h^{i+1} - \boldsymbol{m}_h^i\rangle\Big).
\end{aligned}
$$

Next, we again exploit Lipschitz continuity and Young's inequality to see, for any $\varepsilon > 0$,

$$
\begin{aligned}
&\sum_{i=0}^{j-1}\Big(\langle H_h(\boldsymbol{m}_h^{i+1}) - H_h(\boldsymbol{m}_h^i), \boldsymbol{m}_h^i\rangle - \langle H_h(\boldsymbol{m}_h^i), \boldsymbol{m}_h^{i+1} - \boldsymbol{m}_h^i\rangle\Big) \\
&\qquad\qquad \le 2C_L\sum_{i=0}^{j-1}\|k\boldsymbol{v}_h^i\|_{\boldsymbol{L}^2(\Omega_1)}\Big((C_L + C_{13})|\Omega_1|^{1/2} + \|\boldsymbol{f}_h^j\|_{\boldsymbol{L}^2(\Omega_1)}\Big) \\
&\qquad\qquad \lesssim 2\varepsilon k\sum_{i=0}^{j-1}\|\boldsymbol{v}_h^i\|^2_{\boldsymbol{L}^2(\Omega_1)} + \frac{C_{14}k}{\varepsilon}\sum_{i=0}^{j-1}\|\boldsymbol{f}_h^i\|^2_{\boldsymbol{L}^2(\Omega_1)} + \frac{C_{15}}{\varepsilon}.
\end{aligned}
$$

Here, $C_L > 0$ denotes the Lipschitz constant of $\boldsymbol{\pi}_h$ and $C_{14} = \frac{2C_L^2}{4}$. Therefore, we get

$$\mathcal{E}(\boldsymbol{m}_h^j) + 2k(\alpha - \varepsilon)\sum_{i=0}^{j-1} \|\boldsymbol{v}_h^i\|^2_{\boldsymbol{L}^2(\Omega_1)} \leq \mathcal{E}(\boldsymbol{m}_h^0) + Ck\Big(\|\boldsymbol{v}_{hk}^-\|_{\boldsymbol{L}^2(\Omega_\tau)}\|\nabla \boldsymbol{v}_{hk}^-\|_{\boldsymbol{L}^2(\Omega_\tau)} + \|\boldsymbol{v}_{hk}^-\|^2_{\boldsymbol{L}^2(\Omega_\tau)}\Big) + \frac{C_{14}}{\varepsilon}\|\boldsymbol{f}\|^2_{\boldsymbol{L}^2(\Omega_\tau)} + \frac{C_{15}}{\varepsilon}.$$

For any measurable set $\mathfrak{T} \subseteq [0, \tau]$, we thus conclude

$$\int_{\mathfrak{T}} \mathcal{E}\Big(\boldsymbol{m}_{hk}^+(t)\Big) + 2(\alpha - \varepsilon)\int_{\mathfrak{T}} \|\boldsymbol{v}_{hk}^-\|^2_{\boldsymbol{L}^2(\Omega_t)} \leq \int_{\mathfrak{T}} \mathcal{E}(\boldsymbol{m}_h^0) + Ck\int_{\mathfrak{T}} \|\boldsymbol{v}_{hk}^-\|_{\boldsymbol{L}^2(\Omega_\tau)}\|\nabla \boldsymbol{v}_{hk}^-\|_{\boldsymbol{L}^2(\Omega_\tau)} + Ck\int_{\mathfrak{T}} \|\boldsymbol{v}_{hk}^-\|^2_{\boldsymbol{L}^2(\Omega_\tau)} + \int_{\mathfrak{T}} \frac{C_{14}}{\varepsilon}\|\boldsymbol{f}\|^2_{\boldsymbol{L}^2(\Omega_\tau)} + \int_{\mathfrak{T}} \frac{C_{15}}{\varepsilon}.$$

Passing to the limit as $(h, k) \to (0, 0)$, we finally see

$$\int_{\mathfrak{T}} \mathcal{E}\Big(\boldsymbol{m}(t)\Big) + 2(\alpha - \varepsilon)\int_{\mathfrak{T}} \|\boldsymbol{m}_t\|^2_{\boldsymbol{L}^2(\Omega_t)} \leq \int_{\mathfrak{T}} \mathcal{E}\Big(\boldsymbol{m}(0)\Big) + \int_{\mathfrak{T}} \frac{C_{14}}{\varepsilon}\|\boldsymbol{f}\|^2_{\boldsymbol{L}^2(\Omega_\tau)} + \int_{\mathfrak{T}} \frac{C_{15}}{\varepsilon}.$$

where we have used weak lower semi-continuity on the left-hand side and strong limits on the right-hand side. In addition, we have used the boundedness of $\sqrt{k}\|\nabla \boldsymbol{v}_{hk}^-\|_{\boldsymbol{L}^2(\Omega_\tau)}$ and $\|\boldsymbol{v}_{hk}^-\|_{\boldsymbol{L}^2(\Omega_\tau)}$. Since $\mathfrak{T} \subseteq [0, T]$ was arbitrary, we derive the desired result (80). The extended estimate (81) finally follows from the fact that for vanishing field $\boldsymbol{f}$ and self-adjoint operators $\boldsymbol{\pi}_h$, the term

$$\langle H_h(\boldsymbol{m}_h^{i+1}), \boldsymbol{m}_h^i\rangle - \langle H_h(\boldsymbol{m}_h^i), \boldsymbol{m}_h^{i+1}\rangle$$

in (82) vanishes. This concludes the proof. $\square$

Remark 30. (i) *In a 2D setting, the assumption on the boundedness of $\boldsymbol{\pi}_h(\cdot)$ in $\boldsymbol{L}^4(\Omega_1)$ can be avoided due to the better Sobolev embedding $\|\boldsymbol{v}_h^i\|_{\boldsymbol{L}^4(\Omega_1)} \lesssim \|\boldsymbol{v}_h^i\|_{\boldsymbol{H}^1(\Omega_1)}\|\boldsymbol{v}_h^i\|_{\boldsymbol{L}^2(\Omega_1)}$. In this case, one thus only needs boundedness in $\boldsymbol{L}^2(\Omega_1)$.*
(ii) *The operator $\pi_h(\cdot)$ is, in particular, self-adjoint for a uniaxial anisotropy density, for the strayfield contribution of Section 4.5 as well as for the multiscale contribution of Section 4.6 with linear material law.*

Acknowledgements The authors acknowledge financial support through the WWTF project MA09-029, the FWF project P21732, the FWF project SFB-ViCoM F4112-N13, and the *innovative projects* initiative of TU Wien.

References

[1] F. Alouges: *A new finite element scheme for Landau-Lifchitz equations*, Discrete Contin. Dyn. Syst. Ser. S **1** (2008), 187–196.

[2] F. Alouges, E. Kritsikis, J.-C. Toussaint: *A convergent finite element approximation for Landau-Lifshitz-Gilbert equation*, Physica B, published online first (2011).

[3] F. Alouges, A. Soyeur: *On global weak solutions for Landau-Lifshitz equations: existence and nonuniqueness*, Nonlinear Anal. **18** (1992), 1071–1084.

[4] M. Aurada, M. Feischl, T. Führer, M. Karkulik, J.M. Melenk, D. Praetorius: *Classical FEM-BEM coupling methods: nonlinearities, well-posedness, and adaptivity*, Comp. Mech., in print (2012).

[5] L. Banas, S. Bartels, A. Prohl: *A convergent implicit finite element discretization of the Maxwell-Landau-Lifshitz-Gilbert equation*, SIAM J. Numer. Anal. **46** (2008), no. 3, 1399-1422.

[6] S. Bartels, A. Prohl: *Convergence of an implicit finite element method for the Landau-Lifshitz-Gilbert equation*, SIAM J. Numer. Anal. **44** (2006), no. 4, 1405–1419.

[7] S. Bartels, J. Ko, A. Prohl: *Numerical analysis of an explicit approximation scheme for the Landau-Lifshitz-Gilbert equation*, Math. Comp. **77** (2008), no. 262, 773–788.

[8] F. Bruckner, C. Vogler, M. Feischl, T. Führer, M. Page, D. Praetorius, B. Bergmair, T. Huber, M. Fuger, D. Suess: *Combining micromagnetism and magnetostatic Maxwell equations for multiscale magnetic simulation*, work in progress (2012).
[9] I. Cimrak: *A survey on the numerics and computations for the Landau-Lifshitz equation of micromagnetism*, Arch. Comput. Methods Eng. **15** (2008), no. 3, 277–309.
[10] D.R. Fredkin, T.R. Koehler *Hybrid method for computing demagnetizing fields*, IEEE Trans. Magn. Vol. **26**, No. 2 (1990), 415–417
[11] A. Friedman: *Partial differential equations*, Holt, Rinehart & Winston, New York, 1969.
[12] M. Feischl, M. Karkulik, M. Melenk, D. Praetorius: *Quasi-optimal convergence rate for an adaptive boundary element method*, ASC Report **28** (2011), Institute for Analysis and Scientific Computing, Vienna University of Technology.
[13] C.J. García-Cervera *Numerical micromagnetics: a review*, Bol. Soc. Esp. Mat. Apl. SeMA no. **39**, (2007), 103–135.
[14] P. Goldenits: *Konvergente numerische Integration der Landau-Lifshitz-Gilbert Gleichung*, PhD thesis (in German), Institute for Analysis and Scientific Computing, Vienna University of Technology, 2012.
[15] P. Goldenits, G. Hrkac, M. Mayr, D. Praetorius, D. Suess: *An effective integrator for the Landau-Lifshitz-Gilbert equation*, Proceedings of Mathmod 2012 Conference.
[16] P. Goldenits, D. Praetorius, D. Suess: *Convergent geometric integrator for the Landau-Lifshitz-Gilbert equation in micromagnetics*, Proc. Appl. Math. Mech. **11** (2011), 775–776.
[17] A. Hubert, R. Schäfer: *Magnetic Domains. The Analysis of Magnetic Microstructures*, 1st ed. 1998. Corr. 3rd printing, 1998, Springer, Heidelberg, 1998.
[18] G. Hsiao, W. Wendland: *Boundary integral equations*, Applied Mathematical Sciences 164, Springer-Verlag, Berlin, 2008.
[19] C. Johnson, J.-C. Nédélec: *On the coupling of boundary integral and finite element methods*, Math. Comp. **35** (1980), 1063–1079.
[20] M. Kruzik, A. Prohl: *Recent developments in the modeling, analysis, and numerics of ferromagnetism*, SIAM Rev. **48** (2006), no. 3., 439–483.
[21] W. McLean: *Strongly elliptic systems and boundary integral equations*, Cambridge University Press, Cambridge, 2000.
[22] A. Prohl: *Computational micromagnetism*, Advances in Numerical Mathematics. B. G. Teubner, Stuttgart, 2001.
[23] J. Rivas, J.M. Zamarro, E. Martín, C. Pereira: *Simple approximation for magnetization curves and hysteresis loops*, IEEE Trans. Magn., **17** (1981), 1498–1502.
[24] S. Sauter, C. Schwab: *Boundary element methods*, Springer Verlag, Berlin, 2011.
[25] F.-J. Sayas *The validity of Johnson-Nédélec's BEM-FEM coupling on polygonal interfaces*, SIAM J. Numer. Anal. **47** (2009), 3451–3463.
[26] L.R. Scott, S. Zhang: *Finite element interpolation of nonsmooth functions satisfying boundary conditions*, Math. Comp., **54** (1990), 483–493.
[27] O. Steinbach: *Numerical approximation methods for elliptic boundary value problems: Finite and boundary elements*, Springer, New York, 2008.
[28] R. Verfürth: *A review of a posteriori error estimation and adaptive mesh-refinement techniques*, Teubner, Stuttgart, 1996.
[29] E. Zeidler: *Nonlinear functional analysis and its applications, part II/B*, Springer, New York, 1990.

Institute of Solid State Physics, Vienna University of Technology, Wiedner Hauptstrasse 8-10, A-1040 Wien, Austria

E-mail address: {Florian.Bruckner,Dieter.Suess}@tuwien.ac.at

Institute for Analysis and Scientific Computing, Vienna University of Technology, Wiedner Hauptstrasse 8-10, A-1040 Wien, Austria

E-mail address: {Michael.Feischl,Thomas.Fuehrer,Marcus.Page,Dirk.Praetorius}@tuwien.ac.at